Reviewer Comments for:
Snowmelt response to simulated warming across a large elevation gradient, southern Sierra Nevada, California
By Musselman et al.
Submitted to The Cryosphere

The authors provide a new approach to addressing projected climate impacts on mountain snowpack by focusing on snowmelt. Most previous studies have focused on snowpack. Their perspective is relevant, especially for water management.

Overall the structure of the paper was well organized and presented, and the conceptual design and research is worthy of publication. Before this research is publishable I have one major concern regarding the lack of detail and specifics of the modeling for meteorological conditions and validation of snowpack.

Thank you for your review. We appreciate the recognition of our paper's contribution and scientific relevance. Your support of the ultimate publication of the paper is encouraging. We have addressed suggestions and comments below. Our responses are provided in blue font. References to line numbers refer to those of the revised manuscript.

From the paper I inferred that the authors modeled snowpack using all of the available meteorological stations, but did not validate the meteorological outputs. For example, the authors state "Interpolations were conducted with the data access and pre-processing library MeteoIO [Bavay and Egger, 2014] and computed with an Inverse Distance Weighting (IDW) algorithm with elevation lapse rate adjustments for air temperature, wind speed, and precipitation."

The authors had 19 stations of meteorological forcing data. But were any used to assess the meteorological outputs before calibrating snowpack?

If not the authors calibrated a model to three snow years and then applied projected increased temperatures. If this is the case, their approach is problematic. It is critical to ensure that you are getting modelled results correct for the right reasons (Kirchner, 2006). Modeling snowpack without ensuring that you have the underlying meteorological conditions correct is problematic, because any modeled error propagates through the climate projections. It is pertinent to get the right answers for the right reasons and demonstrate this to the reader.

In my opinion this paper should not be published until the authors clarify their approach or remove some of the forcing stations and use them to validate the meteorological outputs.

We clarify our modeling and validation approaches with three main points A), B) and C). Associated changes to the manuscript are detailed below each point.

A) Unlike a temperature index snowmelt model or a hydrologic model, energy balance snowmelt models are not commonly calibrated. As such, no calibration of the meteorological interpolation procedures or snow model was performed. This approach

relies on the idea that a model based on good understanding of the physical principles and basin characteristics, with an appropriate structure, spatial resolution and parameter selection, should have a good chance of simulating the hydrological cycle including snow accumulation (Pomeroy et al., 2007).

The use of an uncalibrated physically based model requires carefully selected parameters and verification data to ensure model accuracy and characterize model error. This lends confidence that we get the "right answers for the right reasons". For example, "The combination of targeted field observations and uncalibrated physically-based model diagnosis can provide for rapid advances in the understanding of hydrological systems and is recommended for the transfer of scientific understanding to ungauged or poorly gauged basins where calibration is not normally possible." -Pomeroy et al. (2007)

In this vein, we leverage a substantial dataset of diverse field observations. Particularly, we verify the snow model with data from manual plot- and basin-scale SWE surveys that are geographically distant from the local meteorological stations used to force the model. Such validation provides a fairer model skill assessment than the use of SNOTEL SWE observations, which are typically co-located with meteorological stations where errors due to meteorological interpolation should (theoretically) be lowest.

CHANGES: With regard to calibration, we have added the following on Lines 137-138:

"The physically based model system was uncalibrated. Model decisions and parameters were chosen based on their successful application in previous studies."

With regard to model verification and meteorological forcing stations, we have added the following on Lines 538-541 (changes in bold):

"Notwithstanding, there are inherent strengths and weaknesses of the different validation data sets. **For example, automated SWE stations were often co-located with meteorological stations used to force the model; thus, the full potential for model error may not be evaluated at these locations. A fairer model assessment is possible when using data from the plot- and basin-scale snow surveys, which can be further from the local meteorological stations.**"

B) We agree with the Reviewer that errors in spatial meteorological forcing fields can be significant. In fact, we conclude on Lines 548-550 (changes in **bold**) that "Overall, the model performed best in regions closest to precipitation gauges used to force the model (Fig. S1) and tended to slightly overestimate SWE at upper elevations (Table S3) **where no precipitation measurements are available**".

While resulting error in the baseline runs will "propagate through the climate projections", our characterization of problematic regions and times improves our ability to interpret our results. This is stated on Lines 529-530: "Improved model error characterization for the baseline (nominal) years is a critical step toward informed interpretation of the results of our climate change sensitivity analysis."

C) The pre-processing library MeteoIO is an onboard component of the Alpine3D model system. The sensitivities of Alpine3D results to meteorological data coverage, and interpolation and model decisions are thoroughly addressed in Schlögl et al., (2016). The sensitivity of a physically based snow model to errors in forcing input is addressed in Raleigh et al. (2015). Additional assessment is beyond the scope of our study.

CHANGES: The following sentences have been added on Lines 188-189: "The sensitivity of Alpine3D results to meteorological interpolation and model decisions are addressed in *Schlögl et al.,* [2016]."

References:

Pomeroy, J. W., Gray, D. M., Brown, T., Hedstrom, N. R., Quinton, W. L., Granger, R. J., & Carey, S. K. (2007). The cold regions hydrological model: a platform for basing process representation and model structure on physical evidence. *Hydrological processes*, *21*(19), 2650-2667.

Schlögl, S., Marty, C., Bavay, M., & Lehning, M. (2016). Sensitivity of Alpine3D modeled snow cover to modifications in DEM resolution, station coverage and meteorological input quantities. *Environmental Modelling & Software*, *83*, 387-396.

Raleigh, M. S., Lundquist, J. D., & Clark, M. P. (2015). Exploring the impact of forcing error characteristics on physically based snow simulations within a global sensitivity analysis framework. *Hydrology and Earth System Sciences*, *19*(7), 3153-3179.

Other specific comments:

Line 1: The abstract is very well written, with the exception of the first sentence. I did not understand your point until I read the sentence three times. Please consider restructuring it so that there is little to no ambiguity.

We have re-worded the first sentence of the abstract (changes in **bold**):

"In a warmer climate, the fraction of annual meltwater produced at high melt rates **in mountainous areas is** projected to decline due to a contraction of the **snow-cover season, causing melt to occur earlier and under lower energy conditions**."

Lines 90 – 93: I like your description of why you chose only to change changes in temperature.

Thank you.

Line 143: You describe that the model has an arbitrary number of layers. I found myself wanting more information about how the number of layers is/was decided. By the modeler or the model?

The number of snow layers is determined by the model. These model decisions are based on meteorological conditions during snowfall and simulated metamorphic processes (similar neighboring layers may be combined) and melt processes (layers may be removed as they melt). This is a now a common functionality in detailed snow models. We have decided to remove this sentence since 1) the model is described in detail in the Bartelt and Lehning (2002) citation, and 2) the number of snow layers is not directly relevant to our study or results.

Lines 242-243: How were the automated SWE measurements evaluated? This should be provided in the methods.

This is now clarified (changes in **bold**): Modeled SWE fields were evaluated against these station observations **using the RMSE and bias metrics described above**.

Lines 281 – 282: This is a very informative way to organize the elevation bands!

Thank you.

Lines 327 – 329: Please provide some of the result values for Snow Disappearance Date.

We do not quantitatively evaluate snow disappearance date in this study. We believe the (simulated) snow disappearance dates, averaged over elevation bands, are best visualized in Figure 5.

We use the metric to draw relative comparisons between years; however, an arithmetic average will have little physical meaning. We have expanded our description of inter-annual differences in snow disappearance date on Lines 322-326 (changes in **bold**):

"The AMJ period in the moderately wet year was > 2°C colder than the other years (Table 2) due to a series of large snowfall events in mid-April (Fig. 3) that prolonged snow-cover **well into June** (see Figs. 2 **and 3**). **By comparison, snow-cover measured at the automated SWE stations generally disappeared in May in both the drier and average years (Fig. 3).**"

Lines 341 – 346: There are a lot of generalities (i.e. in general is used two times in three sentences). It would be informative to have to have detailed values and let the reader decide in general or not. In its present form, the reader simply has to assume what the authors are telling them with minimal supporting data/evidence.

These terms have been removed. We provide quantitative RMSE and bias metrics for the automated SWE stations and snow survey data. We used general terms to describe simulated snow depth relative to the envelope of measurements from six sensors each within four different model grid cells. We note that:

"Compared to the range of snow depth measured by six sensors at each of four sites in the forested Wolverton basin, the model accurately captured the seasonal snow depth dynamics, including maximum accumulation, the rate of depletion, and the date of snow disappearance (Fig. 4; note that simulated snow depth is generally within the measurement envelope)."

As shown in Fig. 4, there are very few exceptions to this statement, making it generally true.

Lines 359 – 361: I did not see the step-wise jump that you all are referring to here. I fully assume it is my error, but it might be helpful to annotate the jumps for your readers.

We now clarify how we interpret step-wise jumps from figure (changes in **bold**):

"Generally, maximum SWE occurred later with increasing elevation but progressed in a step-wise manner, often with little change over hundreds of vertical meters interspersed with abrupt jumps of one to two months (Fig. 5**; note the occasional large horizontal spacing between 'x' markers of adjacent elevation bands**)"

Lines 368 – 375: This is great data, and well organized.

Thank you.

Lines 445 – 455: This is an important policy/infrastructure component of this work. Consider adding an even more bold statement here. Something along the lines of: "The shift of SWE towards higher unmonitored elevations highlights the need for expanding the existing monitoring network to better manage water resources. For example, in the extremely low snow year of 2015, 1 March 47% of snow monitoring sites in the Willamette River basin, Oregon registered zero SWE, while snow was still present at higher elevations. (Sproles et al., 2017)".

Use the citation or not, but I recommend a stronger policy statement regarding the absence of SWE monitoring at higher elevations, and how the addition of these sites would be critical to monitor snowmelt response to warmer temperatures and for water resource management. Your efforts demonstrate why additional monitoring is important.

Thank you for the reference suggestion. We have added it:

"The results confirm previous findings in the U.S. Pacific Northwest that the current observing network design may be insufficient in a warmer world [Gleason et al., 2017; **Sproles et al., 2017**]."

Since our simulations are limited to three years and three stations, we believe this paragraph adequately communicates our findings, with relevant references to more comprehensive studies, and that further emphasis is not warranted.

Lines 481 – 483: This statement is an important discussion point that could be made stronger by adding a more recent citation and examples from the winters of 2014 and 2015.

We have added reference to a paper by Barnett and Pierce (2009):

Barnett, T. P., and D. W. Pierce (2009), Sustainable water deliveries from the Colorado River in a changing climate, Proceedings of the National Academy of Sciences, 106(18), 7334-7338.

We are not aware of any studies that have explicitly evaluated dam management decisions, particularly, winter water releases and impacts on summer storage, for the two years that the Reviewer suggests.

Lines 519 – 520: Throughout the paper I was expecting snowmelt lysimeters to be included, as either data or as discussion topic. I found the absence of any discussion of lysimeters in a paper focused on snowmelt to be incomplete. Are there no lysimeters in the study area? If not would this also be an infrastructure recommendation? At the minimum, I would suggest a brief explanation of how lysimeters could or could not improve the scientific understanding of snowmelt processes.

This is an excellent point. To our knowledge, there are no snowmelt lysimeters in Sequoia National Park. The data signal from a snowmelt lysimeter would inherently include both snowmelt runoff and rainfall that infiltrates and exits the snowpack. The daily snowmelt signal could be isolated if co-located with a precipitation gauge to extract rainfall response from the record. Measured daily SWE depletion from snow pillows is arguably a more direct estimate of snowmelt rate.

It is unclear how well snowmelt lysimeters work on steep slopes representative of mountainous watersheds. Also, lysimeters may work well at lower to middle elevations in maritime climates where the soil remains unfrozen, but problems have been reported in colder regions / higher elevations where sub-freezing soil-surface temperatures can cause ice to obstruct buried tipping buckets.

We have added the following sentence to Lines 514-516: "While not available in this region, snowmelt lysimeters may be useful additions to long-term research sites to better characterize variability and trends in the flux of water to the soil system."

Lines 529 – 531: This is a pretty critical point, especially since one of your primary findings is that the higher elevation snowpack will be more important under warmer conditions. The fact that the model performs better near forcing stations further supports my concerns modeled temperature and precipitation data not being calibrated/validated. This is an important component of modeling distributed snowpack. Doing so could perhaps improve model performance at higher elevations.

Thanks. Please see our associated response to the Reviewer's primary comment.

We now tie our model uncertainty at higher elevations to the Reviewer's previous point about a need to guide monitoring network design in a warmer climate (changes in **bold**):

Lines 548-553: "Overall, the model performed best in regions closest to precipitation gauges used to force the model (Fig. S1) and tended to slightly overestimate SWE at upper elevations (Table S3) **where no precipitation measurements are available**. **The results complement our**

finding that the current precipitation and snowpack observation network may be insufficient in a warmer world where the majority of snow water resources shifts to higher, unmonitored elevations where snow model error is greatest."

Figure 2: Your color ramp for snow is counterintuitive. Red usually represents warning/drier conditions, but here it represents more snow. Additionally, if you are displaying sequential data it should be on a single color ramp.

This may be an issue of personal preference. In our color scheme, brighter / warmer colors are associated with higher values. An example of NASA using such a color scheme to map precipitation across the United States is provided below (https://www.nasa.gov/feature/goddard/2016/nasa-maps-el-ninos-shift-on-us-precipitation). My feeling is that as long as the color bar index is clear, and colors are easily distinguishable, then the color scheme used to visualize the data is effective.

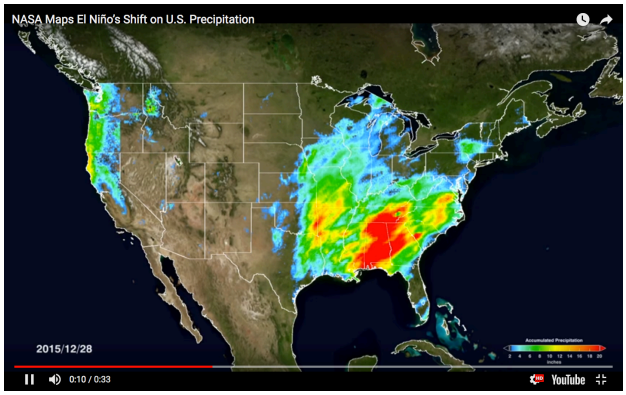

Light, Adam, and Patrick J. Bartlein. "The end of the rainbow? Color schemes for improved data graphics." Eos 85.40 (2004): 385-391.
Also, http://colorbrewer2.org/, has color schemes that work really well. I believe there is a Matlab function for Colorbrewer as well.
https://www.mathworks.com/matlabcentral/fileexchange/34087-cbrewer---colorbrewerschemes-for-matlab

Figure 5: Again, colors are counterintuitive and should be redesigned.

Please see our response to the previous comment.

Figures 6, 7, and 10 are really informative. They provide a lot of information!

Thank you for the detailed and supportive review.

Interactive comment on "Snowmelt response to simulated warming across a large elevation gradient, southern Sierra Nevada, California" by Keith N. Musselman et al.

B. Henn (Referee)
bhenn@ucsd.edu
Received and published: 8 September 2017

General Comments

This study examines the effect of projected climate warming on snow accumulation and melt rates along an elevation gradient and between wet and dry years. The authors use detailed snow and meteorology observations from Sequoia National Park to validate and drive physically based snow model simulations of historic and projected snowpack under warming. The simulations show that historic conditions are reproduced for three years of data with acceptable agreement to observations. They then show sensitivity of snow volumes and melt rates with elevation and wet/dry years, finding that snow volumes decline with warming at about 10%/degC overall with greater losses in the mid elevation coniferous forests, and that melt rates decline in areas of snow loss as melt now occurs earlier in the year. They also argue that extreme high melt rates increase under warming based on one of the three simulated years in which mid-winter melt events occurred more extensively.

The study reinforces previous work that shifts from snow to rain under warming will result in lower snowpacks in mid-elevation areas, and that the lower, more ephemeral snowpacks will melt more slowly and earlier in the winter. The elevation gradient and three years of varying precipitation are helpful in visualizing those effects across those important dimensions of the mountain hydroclimate, making the study a useful contribution.

The authors' claim that extreme melt rates (defined as high-quantile rates under the historic scenario) may increase under warming is novel and has flood risk implications. This claim may need to be phrased more carefully as the majority of the results presented show melt rates decreasing under almost all warming scenarios, and it also seems possible that the increases in melt rates reported are sensitive to the assumptions of the warming perturbations in this particular study. The authors should perhaps more clearly state some of these caveats.

The paper is well written and clearly organized and has high-quality figures.

Thank you for the thoughtful and supportive review. We address your comments and suggestions below.

Specific Comments

L254-262: The section on how longwave radiation was calculated under the perturbation scenarios is clear in terms of how it was done, but would benefit from more conceptual explanation about why this method is appropriate. For example, this method assumes that both

RH and emissivity of the atmosphere do not change under the warming scenarios. While there is conceptual evidence to support (fairly) similar RH in a warmer climate, emissivity has a dependence on temperature (Flerchinger, G. N., W. Xaio, D. Marks, T. J. Sauer, and Q. Yu (2009), Water Resour. Res., doi:10.1029/2008WR007394.)

Given that the authors cite midwinter melt rates as a key finding later in the study, and longwave has been implicated in driving midwinter melt (Lundquist, J. D., Dickerson-Lange, S. E., Lutz, J. a., & Cristea, N. C. (2013). Water Resources Research, http://doi.org/10.1002/wrcr.20504), justifying the perturbation assumptions around longwave and turbulent energy fluxes might benefit the paper.

We agree that this assumption should be stated and implications discussed. It is important to note that the air temperature influence on LW is by far the most dominant component of the Stefan-Boltzmann equation (effective air temperature is to the power of 4).

We have added the following sentence to the section where we first introduce the longwave radiation perturbation. Lines 265-266: "The *in-situ* atmospheric emissivity is assumed to be constant for the perturbed temperature scenarios."

We also discuss the implications of our assumption in the Discussion section where we discuss sources of uncertainty, and conclude that our results are somewhat conservative (Lines 557-560):

"Furthermore, by not perturbing the measured atmospheric emissivity used in the warmer scenarios, we may underestimate the longwave contribution to snowmelt. Atmospheric emissivity varies as a function of column-integrated temperature, specific humidity, and cloud structure above a site [Flerchinger et al., 2009]."

Thank you for the suggestion of the Flerchinger et al., (2009) citation.

L295-297: The explanation of the quantile analysis of melt rates could perhaps be better. If I am understanding correctly, the 99th percentile (for example) melt rates (over the whole spatial domain and year?) are calculated for the nominal case, and then this is repeated for the warming cases and the melt rates are compared?

We now better describe this analysis with the following sentences on Lines 299 – 303:

"For this analysis, the model domain was divided into three elevation bands: 1500 to 2250 m asl, 2250 to 2800 m asl, and >2800 m asl, and percentiles of daily snowmelt were computed for all grid cells in each elevation band. The analysis was conducted separately for each of the three water years and seven scenarios."

L376-389: Somewhere in the paper, discussion about why drier years were more susceptible snowpack loss to warming than wetter years might be warranted. Given that precipitation is fixed, were snow accumulations reduced more in the dry year because those storms were warmer (rain-snow level closer to mean domain elevation) than in wet years? i.e., is this a general finding or something specific to the storms in those years?

To clarify, we don't characterize the dry year as being particularly sensitive to warming. Rather, the wetter year is more resilient to warming than the other two years (an average and a moderately drier year). We explain this difference by the wetter year having substantially lower seasonal (AMJ) average air temperature; however, we do not explicitly analyze synoptic storm temperatures. While not shown, the series of spring storm events in 2010 (wetter year) were unseasonably cold. As simulated, these storms in spring 2010 brought substantial snowfall to low elevations even in the warmest scenario. Thus the phase change was resilient to simulated warming.

We provide a brief discussion of this on Lines 444-446: "The year with the most snowfall, characterized by late snowfall events and cold spring (AMJ) air temperatures, was slightly more resilient (-9.3% $°C^{-1}$) to warming than the drier or average snow years." These seasonal air temperature metrics are provided in Table 3.

L405-408: Perhaps I am misunderstanding Figure 9, but the statement that "Extreme melt rates (99th percentiles; downward-facing triangles in Fig. 9) actually increase (inferred from markers plotting above the 1:1 line) at elevations > 2800 m asl in all years (top panels) and in the drier year at all elevations (left panels)" doesn't quite seem to follow the data - most of the warming scenarios showed did not show increasing 99th percentile rates for the dry year at low elevations, nor did several of the scenarios for each year the high elevation zone. It is interesting that some extreme melt rates did increase, but focusing only on those scenarios that increased might overstate the robustness of this finding.

Thank you for pointing this out. This sentence has been reworded to clarify that we refer to "a majority of the simulations". In the drier year, the Reviewer is correct that only the top two elevation bands (>2250 m) had a majority of simulations in which the 99^{th} percentile values were above the 1:1 line. Lines 412-415 (changes in **bold**):

"**For a majority of the simulations,** extreme melt rates (99^{th} percentiles; downward-facing triangles in Fig. 9) actually increase (inferred from markers plotting above the 1:1 line) at elevations > 2800 m asl in all years (top panels) and in the drier year at elevations **>2250 m asl**."

This is now an accurate statement supported by the data.

L425: The discussion section could benefit from better organization and potentially using subsections to divide it among topics. The ordering of this section (discussing results, then flood and soil moisture implications, then caveats and other issues) seemed a bit meandering for me as a reader (implications for streamflow and soil moisture, processes which are not tested in this paper, seem like they should go last, for example).

We agree that the Discussion would benefit from reorganization. We have taken the Reviewer's suggestion to divide the Discussion Section into three sub-sections:

4.1. Snowmelt response to simulated warming

4.2. Hydrologic Implications

4.3. Sources of uncertainty and caveats

L545: The mechanisms behind the reduction in snowpack with warming seem like they deserve greater discussion here. If I am understanding the experiment, there are only two mechanisms by which warming reduced meltwater volumes: precipitation falling as rain instead of snow, and increased sublimation. How important are these relative to each other in reducing meltwater volumes? Is increased sublimation significant at all or is it entirely the shift to rain? Some discussion of these mechanisms behind the results might be helpful to placing them in physical context.

We now clarify this point on Lines 576-580 (changes in **bold**):

"**The simulated reductions in snowmelt volume due to increased sublimation are very small compared to reductions caused by the warming induced shift from snow to rain. However,** by not considering blowing snow and subsequent sublimation losses (i.e., overestimating alpine snowpack), we may further underestimate snowpack sensitivity to warming."

Technical Corrections
Figure 1: Having repeated numbering of different types of stations is confusing - consider different ways of numbering sites.

Table 1 and Figure 1 have been updated such that each of the 29 stations / snow courses has a unique identifying number.

Snowmelt response to simulated warming across a large elevation gradient, southern Sierra Nevada, California

Keith N. Musselman[1], Noah P. Molotch[2], and Steven A. Margulis[3]

[1]National Center for Atmospheric Research, Boulder, Colorado, USA

[2]Department of Geography, Institute of Arctic and Alpine Research, University of Colorado, Boulder, USA & Jet Propulsion Laboratory, California Institute of Technology, Pasadena, USA

[3]Department of Civil and Environmental Engineering, University of California, Los Angeles, California, USA

Correspondence to: Keith N. Musselman (kmussel@ucar.edu)

Abstract

In a warmer climate, the fraction of annual meltwater produced at high melt rates in mountainous areas is projected to decline due to a contraction of the snow-cover season, causing melt to occur earlier and under lower energy conditions. How snowmelt rates, including extreme events relevant to flood risk, may respond to a range of warming over a mountain front is poorly known. We present a model sensitivity study of snowmelt response to warming across a 3600 m elevation gradient in the southern Sierra Nevada, USA. A snow model was run for three distinct years and verified against extensive ground observations. To simulate the impact of climate warming on meltwater production, measured meteorological conditions were modified by +1°C to +6°C. The total annual snow water volume exhibited linear reductions (-10% $°C^{-1}$) consistent with previous studies. However, the sensitivity of snowmelt rates to successive degrees of warming varied nonlinearly with elevation. Middle elevations and years with more snowfall were prone to the largest reductions in snowmelt rates, with lesser changes simulated at higher elevations. Importantly, simulated warming causes extreme daily snowmelt (99^{th} percentiles) to increase in spatial extent and intensity and shift from spring to winter. The results offer insight into the sensitivity of mountain snow water resources and how the rate and timing of water availability may change in a warmer climate. The identification of future climate conditions that may increase extreme melt events is needed to address the climate resilience of regional flood control systems.

Keith Musselman 10/12/2017 8:25 AM
Deleted: contraction

Keith Musselman 10/12/2017 8:31 AM
Deleted: melt

Keith Musselman 10/12/2017 8:46 AM
Deleted: to an earlier period of lower energy

Keith Musselman 10/13/2017 3:50 PM
Deleted: remains

Keith Musselman 10/12/2017 8:44 AM
Deleted: critical

1. Introduction

Seasonal snow accumulation and melt in mountainous areas are critical components of the regional hydrologic cycle with important controls on climate, ecosystem function, flood risk, and water resources [*Bales et al.*, 2006; *Barnett et al.*, 2005]. Warmer temperatures are expected to reduce snowpack volume and persistence [*Gleick*, 1987; *Knowles and Cayan*, 2004; *Mote et al.*, 2005] by shifting precipitation from snowfall to rain [*Knowles et al.*, 2006] and causing earlier snowmelt [*Stewart et al.*, 2004]. Studies of historical observations in the western U.S. have identified recent declines in spring snowpack [*Mote et al.*, 2005], diminished snowmelt runoff volumes [*Dettinger and Cayan*, 1995; *McCabe and Clark*, 2005] and earlier spring runoff [*Stewart et al.*, 2004]. Most of these studies have attributed the observed trends to anomalously warm spring and summer temperatures of recent decades. *Fyfe et al.* [2017] report that the recent snowpack declines are not replicable with climate model simulations forced by natural changes alone, but are resolved when both natural and anthropogenic changes are considered.

Keith Musselman 10/13/2017 3:52 PM
Deleted: (i.e., internal variability)

Continued warming is expected. General Circulation Models (GCMs) project increases in global average temperatures ranging from 0.7°C ± 0.4°C to 6.5°C ± 2.0°C for the lowest and highest greenhouse gas emission scenarios, respectively, for the end of the next century [*Stocker et al.*, 2013]. The effects of a warmer climate on the snow-dominated hydrology of the Sierra Nevada, for example, are generally recognized to include higher winter storm runoff and flood risk, and reduced summer low-flows [*Dettinger*, 2011; *Dettinger et al.*, 2004; *Godsey et al.*, 2013; *Knowles and Cayan*, 2002; *Lettenmaier and Gan*, 1990]. It is not well understood how present-day snowmelt rates may respond to the range of projected warmer temperature scenarios and, particularly, how those changes will impact water availability over large elevation gradients.

Elevation is a dominant explanatory variable of mountain snow-cover persistence [*Girotto et al.*, 2014b], ranking in importance above solar radiation and terrain aspect for many basins in the western U.S. [*Molotch and Meromy*, 2014]. Snowpack response to warmer temperatures exhibits strong nonlinear elevation dependencies [*Brown and Mote*, 2009; *Knowles and Cayan*, 2004]. For example, slight warming can cause drastic hydrologic response at lower elevations as rain becomes the predominant hydrologic input and snow-cover becomes seasonally intermittent or negligible [*Hunsaker et al.*, 2012; *Marty et al.*, 2017; *Nolin and Daly*, 2006]. At higher and cooler elevations, snowmelt may remain a substantial component of the annual hydrologic input in a warmer climate, but the timing and rate of melt is altered. Rapid and prolonged spring snowmelt is unique to these mountain environments [*Ernesto Trujillo and Molotch*, 2014]. This efficient runoff generation mechanism [*Barnhart et al.*, 2016] produces water resources of vast economic importance [*Sturm et al.*, 2017]. Improved understanding of regional elevation-dependent snowmelt response to warming is a key step toward better predicting and interpreting model estimates of basin-wide runoff.

In a warmer climate, the fraction of meltwater produced at high melt rates is projected to decrease due to a contraction of the historical melt season to a period of lower available energy [*Musselman et al.*, 2017]. Because streamflow is a nonlinear response to hydrologic input, slight reductions in snowmelt rates may disproportionately reduce runoff. Despite recent advances in process understanding, the sensitivity of snowmelt rates to a range of potential warming over a foothills-to-headwaters elevation profile remains poorly known. The topic is a key determinant of changes in how precipitation is partitioned amongst soil storage, evapotranspiration, and runoff with implications on ecological response [*Tague and Peng*, 2013; *Ernesto Trujillo et al.*, 2012] and regional water resources [*Gleick and Chalecki*, 1999; *Vano et al.*, 2014].

We present a climate sensitivity experiment to investigate how carefully-verified model simulations of historical snow water equivalent (SWE) and melt rates respond to successively warmer temperatures that span the range of projected wintertime warming over western North America for this century [*Van Oldenborgh et al.*, 2013]. A controlled experiment with a physically based snow model promotes a detailed analysis of the following research questions: 1) How do SWE and snowmelt rates vary with elevation and how do those gradients vary amongst dry, average, and wet snow seasons? and 2) How do historical SWE and snowmelt rates respond to successive degrees of warming?

2. Methods

To evaluate the response of SWE and snowmelt dynamics to warmer temperatures, we conduct a reanalysis of historical snow seasons using the physically based Alpine3D [*Lehning et al.*, 2006] snow model run at 100 m grid spacing over a mountainous region spanning a 3600-m elevation gradient in the southern Sierra Nevada, California. Snowpack simulations for three historical snow seasons were first verified against multi-scale, ground-based observations. Simulated snowpack characteristics over discrete elevation bands were then examined for their sensitivity to warmer conditions using a delta-change approach in which observed air temperature values and the longwave radiative equivalent were augmented by +1°C to +6°C in +1°C increments. Given the relatively small (< 10%) precipitation changes projected for central and southern California [*Cayan et al.*, 2008], and a lack of agreement of climate models on the sign of projected precipitation changes [*Seager et al.*, 2013], the focus of the current study is on the snowpack response to simulated warming rather than combined changes in temperature and precipitation. Sensitivity was examined for three historical snow years representative of the

102 climatological range in snowfall (years with below-average, average, and above-average
103 snowfall), snow-cover duration, and precipitation timing. The following sub-sections describe
104 the details of our model experiment, verification, and analysis methods.

105 **2.1. Study domain**

106 The study was conducted over a 1648 km^2 area encompassing the 1085 km^2 Kaweah River basin
107 on the western slope of the southern Sierra Nevada, California, USA (36.4ºN, 118.6ºW) (Fig. 1).
108 The elevation of the Kaweah River basin ranges from 250 m to over 3800 m asl. The land-cover
109 and climate of the domain vary substantially over the full 3633 m elevation range (Fig. 1).
110 Approximately 98% of the domain is comprised of four land-cover types [*Fry et al.*, 2011]:
111 conifer forest (58%), shrub (26%), bare soil / rock (10%), and grass / tundra (4%) (Fig. 1). A mix
112 of grassland, shrub, and oak woodlands characterizes the vegetation of the low elevation foothills
113 (< 1600 m asl), where mild and wet winters and arid summers characterize the climate and a 660
114 mm average annual precipitation is rain-dominated [*NPS*, 2017]. At middle elevations (1600 m
115 to 3000 m asl), mixed conifer forest stands are dominant, including some of the world's only
116 giant sequoia (*Sequoiadendron giganteum*) groves. The middle elevation climate is cool with
117 seasonally snow-covered winters and warm, dry summers, and the average annual precipitation
118 exceeds 1080 mm [*NPS*, 2017]. Forest vegetation of the sub-alpine zone, between 3000 m and
119 3500 m asl, is sparse and coniferous. Precipitation is not measured at these upper elevations. At
120 the highest elevations (> 3500 m asl), the land cover is bedrock with sparse alpine vegetation and
121 snow-cover typically persists from November to July.

122 The domain includes two research basins: the 7.22 km^2 forested Wolverton basin and the
123 19.1 km^2 largely alpine Tokopah basin (Fig. 1). The Wolverton basin is representative of

regional forested mid-elevations. A detailed description of the Wolverton basin instrumentation is provided in *Musselman et al.* [2012b]. The 19.1 km^2 Tokopah basin is representative of regional small headwater basins [*Tonnessen*, 1991]. It is instrumented with numerous meteorological stations and has been the subject of many studies on snow distribution [*Elder et al.*, 1988; *Girotto et al.*, 2014a; *Jepsen et al.*, 2012; *Marks et al.*, 1992; *Molotch et al.*, 2005] and biogeochemistry [*Perrot et al.*, 2014; *Sickman et al.*, 2003; *Williams and Melack*, 1991]. We use ground-based observations from these research basins to verify the model as described in Sect. 2.4.

Keith Musselman 10/13/2017 4:02 PM
Deleted: in the southern Sierra Nevada

2.2. Snow model

Alpine3D [*Lehning et al.*, 2006] is a land surface model with an emphasis on snow process representation. It has been used in previous snow process studies [*Bavay et al.*, 2009; *Magnusson et al.*, 2011; *Michlmayr et al.*, 2008; *Mott et al.*, 2008] and projections of future snow or runoff [e.g. *Bavay et al.*, 2013; *Bavay et al.*, 2009; *Kobierska et al.*, 2013; *Kobierska et al.*, 2011; *Marty et al.*, 2017]. At the core of Alpine3D is the one-dimensional SNOWPACK model [*Bartelt and Lehning*, 2002], which has been validated in alpine [e.g. *Etchevers et al.*, 2004] and forested [e.g. *Rutter et al.*, 2009] environments, including a previous study in the Wolverton basin using a subset of the forcing and verification data presented herein [*Musselman et al.*, 2012a]. At each model grid cell, mass and energy balance equations for vegetation, snow, and soil columns are solved with external forcing provided by the atmospheric variables described in Sect. 2.3. The physically based model system was uncalibrated. Model decisions and parameters were chosen based on their successful application in previous studies.

The bottom (soil) boundary conditions were treated with a constant geothermal heat flux of 0.06 W m^{-2} applied at the base of a six-layer soil module [see *Musselman et al.*, 2012a]. In the case of vegetation cover, the surface-atmosphere boundary conditions were solved for in a single-layer canopy module [*Musselman et al.*, 2012a]. Wind transport of snow is not considered in this model implementation. New-snow density and snow albedo parameterizations used in previous studies in the European Alps [*Bavay et al.*, 2013] were found to work well in the Wolverton basin [*Musselman et al.*, 2012a] and are used in the current study. Other land-cover parameters such as canopy height and leaf area index were specified according to land-cover classifications discussed in Sect. 2.3. A simple 1.2°C air temperature threshold was used to distinguish rain from snow, slightly higher than the 1.0°C value used in *Musselman et al.* [2012a].

Keith Musselman 10/13/2017 4:04 PM
Deleted: for more information

Keith Musselman 10/12/2017 8:58 AM
Deleted: The SNOWPACK model treats the snowpack as an arbitrary number of layers.

2.3. Model input data

2.3.1. Topography and land-cover data

The elevation and land-cover across the domain were represented at 100 m grid spacing. Land-cover classification (Fig. 1) was specified from the National Land Cover Database (NLCD) [*Fry et al.*, 2011]. In addition to the land-cover classes listed in Fig. 1, forest-covered grid cells were aggregated into coniferous, mixed, and deciduous categories based on the dominant species within each cell. The NLCD canopy density values, used to parameterize canopy snow interception and snow surface energy fluxes, were binned from 5% to 85% in 10% intervals. Grid elements containing vegetation were specified to have an effective leaf area index and canopy height, respectively, of 0.5 m^2 m^{-2} and 1.5 m for shrub/chaparral, 1.2 m^2 m^{-2} and 20 m for deciduous, 2.0 m^2 m^{-2} and 30 m for mixed, and 2.7 m^2 m^{-2} and 40 m for coniferous forests.

2.3.2 Meteorological data

Hourly meteorological observations were available from 19 stations within the domain (Fig. 1 and Table 1). Sixteen stations recorded hourly air temperature and six reported precipitation (Table 1). The Ash Mountain station at 527 m asl provided the only low elevation precipitation measurements. The Lower Kaweah, Atwell, Giant Forest, and Bear Trap Meadow stations are located within a narrow elevation band of 1926 to 2073 m asl (Fig. 1 and Table 1). Data from a single higher station (Hockett Meadow; 2592 m asl) were not used because of gauge error for the time period of interest. Precipitation gauge catch efficiency was specified as 0.95 for rain and 0.6 for snow, using the 1.2°C air temperature threshold as a determinant of precipitation phase. Incoming shortwave radiation was provided from the Topaz Lake meteorological station (Fig. 1; Table 1). The direct beam was adjusted for grid cell-specific terrain shading and elevation dependency and the diffuse component was assumed spatially uniform for each time step [see *Bavay et al.*, 2013 for details]. The shortwave radiation data are well-correlated with measurements at middle elevations [*Musselman et al.*, 2012b] and are used to model the full domain.

The remaining meteorological variables required spatial interpolation from station locations to all grid cells. Because elevation can have a profound influence on many of the meteorological variables, several of the interpolation methods used linear elevation trends. Interpolations were conducted with the data access and pre-processing library MeteoIO [*Bavay and Egger*, 2014] and computed with an Inverse Distance Weighting (IDW) algorithm with elevation lapse rate adjustments for air temperature, wind speed, and precipitation. Lapse rates were computed for each hourly time step using a regression technique [*Bavay and Egger*, 2014] applied to observations from all available stations. If the correlation coefficient was less than 0.6,

Keith Musselman 10/13/2017 4:06 PM
Deleted: station, and the

195 then a constant elevation lapse rate of -0.008 °C m^{-1} was used for air temperature and a
196 standardized elevation trend of 0.0006 m^{-1} was used for precipitation. The incoming longwave
197 radiation measured at the Topaz Lake station was distributed to all grid cells with a constant
198 elevation lapse rate of -0.03125 W m^{-2} m^{-1} as in *Bavay et al.* [2013]. Relative humidity was
199 interpolated as in *Liston and Elder* [2006]. The sensitivity of Alpine3D results to meteorological
200 interpolation and model decisions are addressed in *Schlögl et al.,* [2016].

201 **2.4. Snow observations and validation data**

202 **2.4.1 Seasonal basin-scale snow surveys**

203 Snow surveys were conducted in the two research basins for three snow seasons: 2008, 2009,
204 and 2010. Three snow surveys of the forested Wolverton basin were conducted each in 2008 and
205 2009. The survey timing coincided with periods of accumulation (mid-February), maximum
206 accumulation (mid-March), and melt (late-April). In all three years, early-April surveys of the
207 alpine Tokopah basin were conducted. In 2009, two additional Tokopah basin surveys captured
208 accumulation (early-March) and melt (mid-May). Surveys were conducted with graduated
209 probes to measure snow depth at waypoint locations on a 250 m grid. Surveyors navigated to the
210 waypoints using Geographic Position System units. At each waypoint, three snow depth
211 measurements separated by five meters were made along a north-south axis. In total over the
212 three years, 1,494 waypoints were surveyed. During each survey, snow density was recorded
213 from snow pits conducted at lower and upper elevations to capture the basin range of snow
214 density; only one snow pit was dug during the 2010 Tokopah survey. An undisturbed snow face
215 was excavated to ground and snow density in duplicate columns was measured in 10 cm vertical
216 intervals by weighing snow samples acquired with a 1000 cm^3 cutter. In total, 26 snow pits were
217 measured over the three years. The average snow density at all pits made during a survey was

used to estimate SWE at waypoint locations, which represent the average of three depth measurements. This approach assumes that basin-scale snow density varies less than snow depth [*López-Moreno et al.*, 2013].

Simulated SWE at model grid-elements containing waypoint positions are evaluated against the snow survey values. Three model evaluation metrics are reported. The model bias is computed as the average difference ('modeled minus measured') of n survey measurements for each waypoint measurement SWE_{o_i} and corresponding model grid cell SWE_{m_i}. The root-mean-square error (RMSE) is computed as

$$\mathrm{RMSE} = \sqrt{\frac{1}{n}\sum_{i=1}^{n}\left(SWE_{m_i} - SWE_{o_i}\right)^2} \qquad \text{Eq. (1)}$$

and the normalized mean square error (NMSE) value is computed as

$$\mathrm{NMSE} = \frac{\overline{(SWE_m - SWE_o)^2}}{\overline{SWE_m}\,\overline{SWE_o}} \qquad \text{Eq. (2)}$$

where the overbars denote the mean over all waypoint locations. The NMSE metric facilitates model performance comparisons amongst basins, months, and years.

2.4.2 Monthly plot-scale snow surveys

Monthly (1 February – 1 May) manual SWE measurements in the Sierra Nevada are made by the California Cooperative Snow Survey (CCSS) program to monitor regional water resources. Seven snow course sites are located within the study domain (Table 1); the sites range in elevation from 1951 m to 2942 m. At each snow course, linear transects of approximately 10 SWE measurements made with Federal snow tube samplers are averaged to represent the mean SWE over a distance similar to the 100 m grid cell spacing. The survey measurements thus

provide a SWE estimate that is arguably more representative of the average value within a corresponding model grid cell than the three point-measurements of the basin-scale surveys or a single automated SWE station measurement. Modeled SWE values for each survey date at the grid cells corresponding to each snow course location were evaluated against measured values.

2.4.3 Automated snow depth sensor network

In addition to the repeated basin- and plot-scale manual snow surveys, the Wolverton basin includes a network of 24 ultrasonic snow depth sensors. Four research sites at different elevations (2253 m, 2300 m, 2620 m, and 2665 m asl) each include six snow depth sensors and each site falls within a different 100 m x 100 m model grid cell. The range of snow depth measured at the six sensors provides a robust estimate of the snow depth, and thus model skill, at four grid cells spanning slope, aspect, forest density, and elevation in the basin.

Keith Musselman 10/13/2017 4:15 PM
Deleted: s

2.4.4 Automated SWE stations

Daily SWE observations were available from three CCSS automated stations (i.e., snow "pillows") at middle elevations: Giant Forest (1951 m asl), Big Meadows (2317 m asl), and Farewell Gap (2896 m) (Table 1 and Fig. 1). Modeled SWE fields were evaluated against these station observations using the RMSE and bias metrics described above. The climatological mean SWE record (26 years at Giant Forest and Big Meadows; 15 years at Farewell Gap) was used to evaluate how the three snow seasons studied here compare to the long-term average.

Keith Musselman 10/12/2017 9:08 AM
Deleted: ‘

Keith Musselman 10/12/2017 9:08 AM
Deleted: pillows’

2.5. Experimental design

The model was run to simulate seasonal snow dynamics for three reference water years (1 October, 2007 – 30 September, 2010) for which the extensive ground-based observations were available. Model estimates of snow depth and SWE were evaluated against the observations.

Six warmer temperature scenarios for each of the three reference years were simulated by increasing the hourly measured air temperature from the 19 regional meteorological stations by +1°C to +6°C in 1°C increments. The lower (+1°C) and upper (+6°C) limits of simulated warming correspond to the average winter air temperature increases projected for the year 2100 in western North America in the Representative Concentration Pathway (RCP) emissions scenarios 2.6 (lowest emissions) and 8.5 (highest emissions), respectively [see top-right panel in Fig. A1.16 in *Van Oldenborgh et al.*, 2013]. For each warmer temperature scenario ($+n$°C) and hourly time step t, the incoming longwave radiation $LW_{\downarrow t}$ [W m^2] measured at the Topaz Lake station was adjusted for the increase in effective radiative temperature resulting from the warmer air. The *in-situ* atmospheric emissivity ϵ_t was estimated from the hourly air temperature T_{a_t} [°C]:

$$\epsilon_t = \frac{LW_{\downarrow t}}{\sigma(T_{a_t}+273.15)^4} \quad \text{Eq. (3)}$$

where σ is the Stefan-Boltzmann constant (5.670373x10^{-8} W m^{-2} K^{-4}). The longwave radiation was adjusted for an effective radiative temperature increase of n [°C] as:

$$LW_{\downarrow t_{(T_a+n)}} = \epsilon_t \sigma (T_{a_t} + 273.15 + n)^4 \quad \text{Eq. (4)}$$

Relative humidity was held constant to allow water vapor pressure to vary in a manner consistent with the ideal gas law [*Rasouli et al.*, 2015]. The *in-situ* atmospheric emissivity is assumed to be constant for the perturbed temperature scenarios. A lack of clear projected wintertime precipitation response to climate change in the southern Sierra Nevada [see Fig. A1.18 in *Van Oldenborgh et al.*, 2013] prompted our focus on temperature sensitivity rather than a

283 combination of temperature and precipitation. Observed and adjusted meteorological variables
284 representative of the warmer scenarios were interpolated to domain grid cells as described in
285 Sect. 2.3.2. The model was run as in the reference scenarios (Sect. 2.2).

286 Daily maps of simulated SWE, snow depth, and sublimation were output for each of the
287 three reference years and six temperature perturbations (21 simulations). For each simulation, we
288 evaluate the elevational distribution of SWE (mm), daily melt (mm day^{-1}), and total annual melt
289 reported as the depth per unit area (mm per 100 m grid cell) and the total volume (km^3). The
290 daily depletion of SWE, less the daily atmospheric exchange with the snow surface (i.e.,
291 sublimation and accretion of ice), is a first-order estimate of daily snowmelt (hereafter, snowmelt
292 rate). The total annual meltwater is then the annual sum of daily snowmelt.

293 To evaluate how SWE and melt in each scenario varied with elevation, metrics were
294 averaged or summed into 200 elevation bands, each encompassing ~18 vertical meters, with a
295 mean of 823 grid cells per elevation band (maximum of 1412). *Rice et al.* [2011] found that
296 snow disappearance in the Sierra Nevada occurred 20 days later for each 300 m rise in elevation.
297 The 18 m elevation discretization captures this variability at approximately one day per elevation
298 band. For each warmer scenario, the total annual meltwater volume is reported as the fraction of
299 that simulated in the nominal (i.e., unperturbed) case. For all scenarios, we report the annual
300 meltwater in three ways: the average meltwater volume and melt rate within each elevation band,
301 the sum of annual meltwater within each elevation band, and the total annual meltwater summed
302 over the entire model domain. The sensitivity of total domain-wide annual meltwater to
303 simulated warming is examined with a (linear) regression analysis of the fraction of historical
304 total meltwater for each warmer scenario of the three years.

To evaluate the effect of simulated warming on melt rates over the elevation profile for the three years, we report the elevation-specific mean fraction of total annual meltwater produced at high ($\geq$ 15 mm day^{-1}) melt rates, reported as a percent change relative to the nominal case. The 15 mm day^{-1} threshold was selected as a compromise between the 12.5 mm day^{-1} threshold above which positive streamflow anomalies were reported by *Barnhart et al.* [2016] and a 20 mm day^{-1} classification of very heavy rainfall [*Klein Tank et al.*, 2009] used by *Musselman et al.* [2017]. To examine how daily snowmelt rates respond to simulated warming, we present a quantile analysis of the 25th, 50th, 75th, 90th, 95th, and 99th percentiles of daily snowmelt rates $\geq$ 1 mm day^{-1} from the warmer scenarios compared to those from the nominal case. For this analysis, the model domain was divided into three elevation bands: 1500 to 2250 m asl, 2250 to 2800 m asl, and >2800 m asl, and percentiles of daily snowmelt were computed for all grid cells in each elevation band. The analysis was conducted separately for each of the three water years and seven scenarios. Lastly, we present an analysis of the meteorological conditions that control the response of snowmelt rates to successive degrees of simulated warming.

3. Results

Maps of simulated SWE on 1 April, 1 May, and 1 June (Fig. 2) highlight seasonal and inter-annual SWE patterns and illustrate the great variability of SWE with elevation. The lowest elevations were consistently snow-free during the spring. Middle elevations included a transition zone from snow-free to seasonally persistent snow-cover; that transition occurred at progressively higher elevations later in the melt season and occurred earlier (later) in the drier (wetter) snow years. The upper elevations contained the greatest SWE and most persistent spring snow-cover (Fig. 2). The three-year observation period captured years with below-average

snowfall (2009; 23% below average SWE; hereafter 'moderately dry year'), average snowfall (2008; 7% above average SWE; hereafter 'average year'), and above-average snowfall (2010; 54% above average SWE; hereafter 'moderately wet year') as determined from regional automated SWE records (Fig. 3 and Table S1). The average (hourly) air temperature and shortwave radiation values measured at the alpine Topaz Lake station in January-February-March (JFM; the accumulation season) and April-May-June (AMJ; the melt season) provides more insight into the meteorological differences amongst the three years. The drier and average years exhibited similar average air temperatures, but the AMJ mean shortwave radiation was lower in the moderately dry year (Table 2) due to higher spring cloud-cover (see Fig. 6 in *Musselman et al.* [2012b]). The AMJ period in the moderately wet year was > 2°C colder than the other years (Table 2) due to a series of large snowfall events in mid-April (Fig. 3) that prolonged snow-cover well into June (see Figs. 2 and 3). By comparison, snow-cover measured by the automated SWE stations generally disappeared in May in both the drier and average years (Fig. 3).

3.1. Model evaluation against observation

Compared to automated snow pillow SWE measurements, the model performed favorably (RMSE ≤ 100 mm; bias better than ±85 mm) at all elevations in 2008 and 2010 (Fig. 3). In 2009, the model underestimated SWE compared to measurements made at the two higher elevation stations, but accurately simulated SWE at the lower Giant Forest station (RMSE = 34 mm; bias = -4 mm) (Fig. 3). The greatest model error occurred in 2009 at the Big Meadows station (2317 m asl) resulting from a significant underestimation of all snow events, possibly due

to sensor error, and errors were less at the higher and lower elevation stations in this year (Fig. 3).

Compared to the range of snow depth measured by six sensors at each of four sites in the forested Wolverton basin, the model accurately captured the seasonal snow depth dynamics, including maximum accumulation, the rate of depletion, and the date of snow disappearance (Fig. 4; note that simulated snow depth is generally within the measurement envelope). The underestimation of SWE in 2009 was not apparent in the verification against the six automated depth measurements at four sites in the Wolverton basin (Fig. 4).

The early-April surveys of the alpine Tokopah basin show 2009, 2008, and 2010 being the drier (849±401 mm SWE), average (1000±476 mm SWE), and wetter (1265±310 mm SWE) snow seasons, respectively (Table S2). Model SWE errors (NMSE) were highest during the melt season when the measured variability was high relative to the mean, and lowest during the accumulation season (Table S2). On average, the forested Wolverton and alpine Tokopah basins exhibited similar NMSE values of ~ 0.14 at maximum accumulation. In general, the model tended to overestimate SWE with the exception of the February 2009 Wolverton survey, for which modeled SWE was negatively biased (Table S2). The survey mean bias values were typically much less than the standard deviation of the biases.

In general, model SWE errors were lower when evaluated against the CCSS snow course measurements (Table S3) than the basin-wide survey measurements (Table S2). The large underestimation of SWE in 2009 seen in the comparison against the automated SWE stations (Fig. 3) is also seen in comparison to SWE measured at the two lowest elevation snow course sites (Table S3). Conversely, comparison to the two highest elevation snow course sites indicated a slight positive model bias in 2009. Overall, the model performed best in regions closest to

Keith Musselman 10/12/2017 10:02 AM
Deleted: and

Keith Musselman 10/12/2017 10:01 AM
Deleted: Despite this underestimation, in general, the SWE magnitude and date of snow disappearance was well approximated by the model compared to the automated station measurements.

Keith Musselman 10/12/2017 10:03 AM
Deleted: general

Keith Musselman 10/13/2017 4:23 PM
Deleted: est

379 precipitation gauges used to force the model; SWE RMSE values were better explained by this
380 metric than by elevation alone (Fig. S1).

381 **3.2. Elevation-dependent SWE and snowmelt patterns**

382 The upper panels of Fig. 5 show the nominal simulations of the daily SWE and melt averaged
383 along elevation bands for the three years. Persistent seasonal snowpack was simulated >1800 m
384 asl in all years. Maximum annual SWE increased with elevation (colors in the top row panels of
385 Fig. 5); however, the date of maximum SWE exhibited a complex relationship with elevation,
386 snowfall magnitude and timing, and snowpack persistence that all varied amongst years (Fig. 5).
387 Generally, maximum SWE occurred later with increasing elevation but progressed in a step-wise
388 manner, often with little change over hundreds of vertical meters interspersed with abrupt jumps
389 of one to two months (Fig. 5; note the occasional large horizontal spacing between 'x' markers
390 of adjacent elevation bands).

391 Simulated daily melt was episodic in nature with the highest rates (> 35 mm day^{-1}; reds in
392 the bottom panels of Fig. 5) generally confined to elevations > 2000 m asl and the late-spring and
393 early summer. The highest elevations and years with more/later snow had the highest melt rates.
394 In all three years, winter melt was generally low (<5 mm day^{-1}) with rare, episodic, and more
395 intense melt events confined to lower elevations (Fig. 5).

396 **3.3. Elevation-dependent snowpack and snowmelt response to warming**

397 In the nominal case, the total meltwater volume summed over each elevation band was
398 consistently greatest between 2500 m and 2800 m asl (see Fig. 6; right panels), corresponding to
399 the peak in the regional hypsometry (see histograms in Fig. 1). Under the warmer scenarios, the

400 maximum meltwater volume, inferred from the peaks in Fig. 6, shifts upward in elevation by ~
401 600 m to the regional treeline (see Fig. 1). This upward elevation shift occurred under +2°C,
402 +3°C, and +4°C warming for the dry, average and wet snow seasons, respectively. Additional
403 warming reduced the total melt volume, but did not change the elevation at which the maximum
404 volume occurred.

405 Lower and middle elevations were prone to large reductions in the fraction of historical
406 meltwater volume (see line graphs in Fig. 6). At 2000 m asl, only 50% of the historical water in
407 the form of snow remained in a +3°C scenario, further reducing to 20% in the +5°C scenario.
408 Overall, snow at the upper elevations in the moderately dry snow season was more susceptible to
409 large reductions (Fig. 6). Conversely, upper elevation snowpack during the average and higher
410 snowfall seasons was more resilient to warming. For example, at 2700 m asl, +1°C warming
411 reduced annual meltwater volume by 1%, 3%, and 11% in the wetter, average and drier snow
412 seasons, respectively; those values increased to 7%, 21% and 28% in the +3°C scenario.

413 Despite elevation-dependent nonlinear meltwater response to warming, the domain-total
414 meltwater volume exhibited linear response to successive warming. Figure 7 shows linear
415 regressions fit to the fraction of the nominal-case total meltwater for each scenario and year (see
416 Table S4). The dry and average years were slightly more susceptible to warming (-10.5% to -
417 10.8% change per °C) than the wetter year (-9.3% change per °C). Sublimation estimates ranged
418 from 5% to 9% in the nominal case to 8% to 14% in the +6°C scenario (Table S4).

419 Warmer temperatures impact not only the total annual meltwater, but also the rate at
420 which meltwater is produced. Figure 8 shows the fraction of the total meltwater per unit area
421 over the elevation profile that is produced at high ($\geq$ 15 mm day^{-1}) melt rates; the complement of
422 that fraction occurs at lower (<15 mm day^{-1}) rates. Consistently, meltwater production at upper

elevations is dominated by high melt rates, while at lower elevations melt rates are predominately low. At ~ 2200 m asl, melt in the nominal cases occurred equally at low and high rates; above this middle elevation zone, melt occurs at high rates (≥ 15 mm day^{-1}) and at low rates (<15 mm day^{-1}) below this elevation (see black circle markers in Fig. 8). Warming greatly decreases the fraction of meltwater produced at high melt rates and increases that produced at low rates (see lower colored graphs in Fig. 8). As a result, the elevation at which meltwater is produced equally at low and high rates is pushed upward by ~150 m $°C^{-1}$ (Fig. 8). The greatest melt rate reductions occur at forested elevations with generally lesser change in alpine areas above ~ 3300 m asl.

There is a general tendency toward lower snowmelt rates in response to successive warming with the lower elevations and the year with the most snowfall (and latest storm events) prone to the greatest reductions (Fig. 9). There are notable exceptions. For a majority of the simulations, extreme melt rates (99^{th} percentiles; downward-facing triangles in Fig. 9) actually increase (inferred from markers plotting above the 1:1 line) at elevations > 2800 m asl in all years (top panels) and in the drier year at elevations >2250 m asl. To better understand why these extreme melt rates differ in trend from the lower percentiles, we provide a brief analysis of 2009 extreme melt events. The analysis is limited to elevations above 2250 m asl where a threshold of 40 mm day^{-1} designates extreme (99^{th} percentiles) melt rates (see Fig. 9).

In the spring, extreme melt affected a very limited portion of the domain on any given day (inferred from blue colors on the right in the top panel of Fig. 10), and the spatial extent of extreme melt generally decreased in response to warming. Conversely, three distinct extreme melt events on 21 January, 22 February, and 1 March 2009 (arrows in Fig. 10) exhibit large increases in the fraction of the domain affected, with the January and March events increasing in

Keith Musselman 10/13/2017 1:00 PM
Deleted: Extreme

Keith Musselman 10/13/2017 1:00 PM
Deleted:

Keith Musselman 10/13/2017 1:00 PM
Deleted: all

Keith Musselman 10/13/2017 1:15 PM
Deleted: (left panels)

spatial extent until +4°C before decreasing with additional warming. The simulated melt events were not associated with substantial rainfall, but rather cloudy and/or windy conditions with high longwave radiation that generally occurred under warmer-than-average temperatures in the nominal case. Measured meteorological conditions for these days are provided in Table 3. These warm and cloudy winter conditions were insufficient to produce widespread extreme melt in the nominal case; melt was limited to elevations < 2000 m asl and generally did not exceed the 99th percentile (Table 3). Additional warming caused extreme rates of melt to occur at increasingly higher elevations at a time of substantial snow-cover (Fig. 10).

4. Discussion

4.1. Snowmelt response to simulated warming

Our results confirm that climate warming will have uneven effects on the California landscape [*Cayan et al.*, 2008] and that elevation is a critical determinant of snowpack – climate sensitivity. Despite the simplicity of our climate sensitivity method, the predicted sensitivity of total snow volume to warming of -9.3% to -10.8% °C^{-1} is consistent with previous studies using either statistical and dynamical downscaling of GCM output (*Sun et al.* [2016]; -9.3% °C^{-1}) or a simple statistical snow model trained on observations (*Howat and Tulaczyk* [2005]; -10% °C^{-1}). The consistency suggests that these models of varying complexity adequately treat the warming-induced shift from snowfall to rain. This confirms recent findings by *Schlögl et al.* [2016] that snow model errors may be less important when relative climate sensitivity metrics are evaluated. Further, we show linearity in the sensitivity of domain-wide annual meltwater volume to successive degrees of warming. The year with the most snowfall, characterized by late snowfall events and cold spring (AMJ) air temperatures, was slightly more resilient (-9.3% °C^{-1}) to

Keith Musselman 10/13/2017 2:05 PM
Formatted: Indent: First line: 0"

Keith Musselman 10/13/2017 2:05 PM
Formatted: Font:Bold

Keith Musselman 10/13/2017 4:32 PM
Deleted: negligible

473 warming than the drier or average snow years. In a study of the sensitivity of snow to warming in
474 Mediterranean climates, including the Tokopah basin, *López-Moreno et al.* [2017] report that
475 simulated changes in precipitation magnitude (±20%) did not affect the relative snowpack
476 climate sensitivity to warming. Thus, snowmelt rates may be more sensitive to changes in the
477 seasonal timing of precipitation than to changes in precipitation magnitude. This supports the
478 conclusions of *Cooper et al.* [2016] that record low snowpack years may not serve as appropriate
479 analogues for the climate sensitivity of snow.

480 In a warmer climate, shifts from snowfall to rain are likely to combine with shifts in
481 snowmelt timing to cause earlier water availability relative to the historical period. As a result,
482 the ephemeral snow zone is expected to progress upward in elevation [*Minder*, 2010] and shift
483 the areal distribution of SWE toward higher, unmonitored elevations. Indeed, the +3°C scenario
484 shifted the elevation of maximum annual meltwater volume above that of the highest regional
485 SWE observing station. The results confirm previous findings in the U.S. Pacific Northwest that
486 the current observing network design may be insufficient in a warmer world [*Gleason et al.*,
487 2017; *Sproles et al.*, 2017]. Warmer temperatures and earlier melt timing [*Stewart et al.*, 2004]
488 also influence the rate of meltwater production [*Musselman et al.*, 2017], a critical determinant
489 of streamflow [*Barnhart et al.*, 2016], forest carbon uptake [*Winchell et al.*, 2016], and flood
490 hazard [*Hamlet and Lettenmaier*, 2007]. Despite a strong negative relationship between
491 temperature and elevation, we show a positive relationship between elevation and seasonal
492 snowmelt rates. Compared to earlier melt at lower elevations, later snowmelt at upper elevations
493 was more rapid due largely to higher solar insolation coincident with later melt [*Musselman et*
494 *al.*, 2012b]. Prolonged snow-cover at upper, compared to lower elevations, and in wetter,

compared to drier snow seasons, is an important factor in interpreting snowmelt temperature sensitivity results.

We show a general tendency toward lower melt rates in response to warming. In contrast to *Musselman et al.* [2017], which evaluated mean snowmelt response to a single greenhouse gas emissions scenario at 4 km resolution, we evaluate a range of potential warming, examine the percentile distribution of snowmelt response, and elucidate the process along elevational gradients most relevant to basin-wide runoff. This is a critical advancement in understanding how and where meltwater production is impacted by warming; an evaluation that cannot be achieved with the type of 'high-resolution' climate modeling used in *Musselman et al.* [2017]. Importantly, we report an emergence (i.e., not present in the historical simulations) and spatial expansion of extreme winter melt events and, conversely, a decline in extreme melt during spring. Increases in extreme winter melt occurred under warm and cloudy conditions, and decreases in extreme spring melt were due to reduced snow-cover persistence. This is an important new finding with implications on flood hazard and reservoir management. The general tendency toward slower snowmelt rates and higher extreme values is analogous to the expected climate change impacts on precipitation, where high-intensity events are expected to increase despite projected declines in total (e.g., summer) precipitation [*Prein et al.*, 2016; *Trenberth*, 2011].

Keith Musselman 10/12/2017 11:48 AM
Deleted: was

4.2. Hydrologic Implications

Keith Musselman 10/13/2017 2:04 PM
Formatted: Indent: First line: 0"

Keith Musselman 10/13/2017 2:04 PM
Formatted: Font:Bold

Increases in extreme winter melt rates, combined with a greater proportion of precipitation falling as rain could locally increase winter flood risk. Higher winter runoff complicates reservoir management faced with competing objectives to maintain flood control storage capacity during winter and to maximize water storage during spring in preparation for the

519 arid summer. In this context, substantial winter runoff may have to be released downstream
520 thereby reducing summer water storage required for agriculture, fish and wildlife management,
521 hydropower production, recreation, water quality and municipal supply [*Barnett and Pierce*,
522 2009; *Lettenmaier et al.*, 1999]. We show that historical extreme melt rates (99th percentiles)
523 impact a relatively limited area (generally <30% of land area above 2250 m asl) at any given
524 time. This is likely due to snowpack cold content and/or cool air temperatures limiting melt at
525 upper elevations and low snow-cover fraction limiting melt at lower elevations. Compared to the
526 historical period, warming doubles the basin area that experiences extreme melt, and shifts its
527 occurrence from spring to winter. The increased spatial extent, intensity, and frequency of
528 extreme winter snowmelt events may have significant implications for antecedent moisture
529 conditions and associated flood risk.

Keith Musselman 10/12/2017 4:36 PM
Deleted: undergoing

530 Snowmelt rates have been mechanistically linked to streamflow production [*Barnhart et*
531 *al.*, 2016], but less-understood are the potential implications of climate-induced changes in
532 snowmelt rates on subsurface water storage, evapotranspiration and streamflow response. For
533 example, recent empirical evidence that a precipitation shift from snow towards rain will lead to
534 a decrease in streamflow [*Berghuijs et al.*, 2014] lacks definitive causation. Compared to soil,
535 snow-cover exhibits different water routing mechanisms. For example, lateral downslope flow of
536 water along snowpack layers has been shown to explain the observed rapid delivery of water to
537 streams and anomalously high contributions of event water to the hydrograph during rain-on-
538 snow and snowmelt [*Eiriksson et al.*, 2013]. One hypothesis is that as snow-cover becomes less
539 persistent in a warmer world, and snowmelt rates decline, this rapid slope-scale redistribution of
540 water toward stream channels will slow or cease, increasing the soil residence time of water.
541 Longer soil residence time can increase the partitioning of water to evapotranspiration, and thus

decrease streamflow. While not available in this region, snowmelt lysimeters may be useful additions to long-term research sites to better characterize variability and trends in the flux of water to the soil system.

Other empirical and modeling studies have reported declines in summertime streamflow due to earlier snowmelt runoff and earlier depletion of shallow aquifers [*Huntington and Niswonger*, 2012; *Luce and Holden*, 2009]. Catchment wetness (i.e., soil moisture content and shallow groundwater levels) has substantial impact on runoff response in mountainous areas with distinct thresholds determining relationships amongst wetness, streamflow, and contributing area [*Penna et al.*, 2011]; behavior controlled by soil type, subsurface storage capacity, and climate. These factors are also important drivers of evapotranspiration [*Christensen et al.*, 2008; *Lundquist and Loheide*, 2011] and the regional variability of hydrologic sensitivity to climate change [*Tague et al.*, 2008]. In this regard, percentage reductions in future streamflow may be more substantial than the meltwater reductions reported here because slower snowmelt is less efficient at generating streamflow.

4.3. Sources of uncertainty and caveats

Improved model error characterization for the baseline (nominal) years is a critical step toward informed interpretation of the results of our climate change sensitivity analysis. While snow model errors may be less important when relative climate sensitivity metrics are evaluated [*Schlögl et al.*, 2016], runoff simulations require accurate representation of snowpack volume and melt rates. Simulated snow depth values were within the range of observations from automated sensors at four sites spanning elevation, forest density, slope and aspect. This verification provides confidence in the model to capture accumulation, melt rates, and the date of snow disappearance across spatial and temporal scales.

Keith Musselman 10/13/2017 2:00 PM
Formatted: Indent: First line: 0"

Keith Musselman 10/13/2017 2:02 PM
Formatted: Font:Bold

Keith Musselman 10/13/2017 4:42 PM
Deleted: negligible

Notwithstanding, there are inherent strengths and weaknesses of the different validation data sets. For example, automated SWE stations were often co-located with meteorological stations used to force the model; thus, the full potential for model error may not be evaluated at these locations. A fairer model assessment is possible when using data from the plot- and basin-scale snow surveys, which can be further from the local meteorological stations. In another example, the plot-scale survey design samples many SWE measurements within a 100-m grid cell, while the basin-scale surveys sampled snow depth at only three measurement points, relying on extrapolation from a few density measurements to estimate SWE. The automated SWE stations only sample a single point. The degree to which these point samples represent the average value over an area consistent with the model grid scale is a source of inherent discrepancy between models and observations, independent of model skill [*Trujillo and Lehning*, 2015]. Overall, the model performed best in regions closest to precipitation gauges used to force the model (Fig. S1) and tended to slightly overestimate SWE at upper elevations (Table S3) where no precipitation measurements are available. The results complement our finding that the current precipitation and snowpack observation network may be insufficient in a warmer world where the majority of snow water resources shifts to higher, unmonitored elevations where snow model error is greatest.

Our assumption of a uniform temperature perturbation does not consider changes in climate dynamics at diurnal (e.g., nighttime vs. daytime temperature changes), synoptic (e.g., number of cool vs. warm days), or seasonal (e.g., winter vs. spring temperature changes) scales. Furthermore, by not perturbing the measured atmospheric emissivity used in the warmer scenarios, we may underestimate the longwave contribution to snowmelt. Atmospheric emissivity varies as a function of column-integrated temperature, specific humidity, and cloud

Keith Musselman 10/11/2017 4:14 PM
Deleted: For example,

Keith Musselman 10/11/2017 4:31 PM
Deleted: design

Keith Musselman 10/11/2017 4:31 PM
Deleted: s only three

Keith Musselman 10/11/2017 4:20 PM
Deleted: within a given grid cell

Keith Musselman 10/11/2017 4:24 PM
Deleted: Similarly, t

structure above a site [*Flerchinger et al.*, 2009]. All of these interactions may be best characterized using GCM output dynamically downscaled to fine-resolutions with regional climate models [e.g., *Liu et al.*, 2016; *Sun et al.*, 2016] or within a delta-change approach that considers the range of uncertainties in the climate change signal of different emissions scenarios [e.g., *Marty et al.*, 2017]. By not addressing the snow-albedo feedback between snow-cover depletion and warmer temperatures [*Letcher and Minder*, 2015; *Pepin and Lundquist*, 2008], it is possible that we underestimate regional air temperature changes toward the end of the melt season in the warmer scenarios. Such negative temperature biases would cause underestimation of the snow depletion rate and, ultimately, the snowpack sensitivity to warming. However, these biases may be partially mitigated by our assumption that the winter and spring, and nighttime and daytime, air temperatures warm uniformly.

Sublimation estimates of 5% to 9% in the nominal case to 8% to 14% in the +6°C scenario (Table S4) are on the lower- to middle-end of the reported regional values of 2% to 3% [*West and Knoerr*, 1959] to 20% [*Marks and Dozier*, 1992]. The large range highlights challenges and disparities in measuring [e.g., *Molotch et al.*, 2007; *Sexstone et al.*, 2016] and modeling [*Etchevers et al.*, 2004] turbulent exchange, which are further compounded in mountainous terrain due to the challenges of windflow simulation [*Musselman et al.*, 2015]. The simulated reductions in snowmelt volume due to increased sublimation are very small compared to reductions caused by the warming induced shift from snow to rain. However, by not considering blowing snow and subsequent sublimation losses (i.e., overestimating alpine snowpack), we may further underestimate snowpack sensitivity to warming.

In light of the potential errors discussed above, our results should be considered somewhat conservative. Longer-term snow and runoff simulations at scales sufficient to resolve

Keith Musselman 10/13/2017 10:43 AM
Deleted: T

Keith Musselman 10/13/2017 2:28 PM
Deleted:

Keith Musselman 10/13/2017 2:29 PM
Deleted: By

621 mountain climate elevation gradients are needed both as reanalysis to understand historical
622 conditions [e.g., snow reanalysis by *Margulis et al.*, 2016], and forced by large suites of future
623 climate scenarios [e.g., *Eyring et al.*, 2016] that dynamically resolve different model realizations
624 of climate response to different greenhouse gas emissions scenarios. Such efforts will best
625 inform, and constrain the uncertainty of, potential impacts of climate change on flood risk and
626 water availability. Toward this goal, our work makes inroads to quantify how snowpack and melt
627 dynamics respond to incremental warming over an elevation profile characteristic of a foothills-
628 to-headwaters mountain front. The results offer insight into the sensitivity of snow water
629 resources to climate change in the Sierra Nevada, California, with implications for other regions
630 as well.

631 **5. Conclusions**

632 We present a climate sensitivity experiment to investigate how historical snow water resources
633 and melt rates respond to successively warmer temperatures over a large elevation gradient in the
634 southern Sierra Nevada, California. Good agreement between simulations and an unprecedented
635 array of ground-based observations of SWE (RMSE $\leq$ 100 mm; bias better than $\pm$85 mm) and
636 snow depth (within multi-sensor range) is shown. Three primary findings emerge from the
637 simulations. First, the sensitivity of total snow-water volume to warming is -9.3% to -10.8% per
638 °C. The snow season characterized by above-average snowfall and cold spring storm events was
639 most resilient to warming; however, it also exhibited the greatest shift toward slower melt. Thus,
640 snowmelt rates may be more sensitive to changes in the seasonal timing of precipitation than to
641 changes in precipitation magnitude. Second, the middle elevations, which are dominated by
642 forest cover and comprise a disproportionately large basin area, exhibit the greatest snowpack
643 reductions and the largest shift toward slower snowmelt. Hence, warming-related impacts on

644 runoff production and ecosystem function may be particularly acute in these areas. Third,
645 increases in the frequency, intensity, and spatial extent of extreme winter melt events occur with
646 successive warming. Warming-induced extreme (winter) melt impacts an area nearly twice as
647 large as that simulated at any time in the historical period. The changes in extreme snowmelt
648 events have implications for antecedent moisture conditions and associated flood risk. When
649 considered together, the elevation-dependent climate sensitivity of snowmelt revealed herein has
650 broad implications for water supply monitoring, streamflow production, flood control, and
651 ecosystem function in a warmer world.

Acknowledgements

The authors thank Sequoia National Park for support of research efforts. Financial support was provided by the National Science Foundation grants EAR-1032295, EAR-1032308, and EAR-1246473, the Southern Sierra Critical Zone Observatory (EAR-0725097), a Major Research Instrumentation grant (EAR-0619947), and the Mountain Research Initiative. The first author was supported by a National Aeronautics and Space Administration (NASA) Earth System Science Fellowship. R. Bales and P. Kirchner supported hydrometeorological infrastructure in the Wolverton basin. J. Sickman and J. Melack provided solar radiation and snow survey data from the Tokopah basin. Alpine3D is provided the WSL Swiss Federal Institute for Snow and Avalanche Research SLF (online: https://models.slf.ch/p/alpine3d/downloads/). Special thanks goes to M. Lehning and M. Bavay. Model forcing data are freely available online from the agencies listed in Table 1. Land-cover and validation data are either available online from sources referenced in the text, or are otherwise provided in the figures, tables, and supplements. The authors are grateful to everyone who provided field assistance including: K. Skeen, S. Roberts, B. Forman, D. Perrot, E. Trujillo, L. Meromy, M. Girotto, A. Kahl, K. Ritger, N. Bair, D. Berisford, A. Kinoshita, and M. Cooper.

668 **References**

669 Bales, R. C., N. P. Molotch, T. H. Painter, M. D. Dettinger, R. Rice, and J. Dozier (2006),
670 Mountain hydrology of the western United States, *Water Resour. Res.*, *42*(8), W08432.
671 Barnett, T. P., and D. W. Pierce (2009), Sustainable water deliveries from the Colorado River in
672 a changing climate, *Proceedings of the National Academy of Sciences*, *106*(18), 7334-7338.
673 Barnett, T. P., J. C. Adam, and D. P. Lettenmaier (2005), Potential impacts of a warming climate
674 on water availability in snow-dominated regions, *Nature*, *438*(7066), 303-309.
675 Barnhart, T. B., N. P. Molotch, B. Livneh, A. A. Harpold, J. F. Knowles, and D. Schneider
676 (2016), Snowmelt rate dictates streamflow, *Geophysical Research Letters*, *43*(15), 8006-8016.
677 Bartelt, P., and M. Lehning (2002), A physical SNOWPACK model for the Swiss avalanche
678 warning: Part I: numerical model, *Cold Regions Science and Technology*, *35*(3), 123-145.
679 Bavay, M., and T. Egger (2014), MeteoIO 2.4. 2: a preprocessing library for meteorological data,
680 *Geoscientific Model Development*, *7*(6), 3135-3151.
681 Bavay, M., T. Grünewald, and M. Lehning (2013), Response of snow cover and runoff to climate
682 change in high Alpine catchments of Eastern Switzerland, *Advances in Water Resources*, *55*,
683 4-16.
684 Bavay, M., M. Lehning, T. Jonas, and H. Löwe (2009), Simulations of future snow cover and
685 discharge in Alpine headwater catchments, *Hydrological Processes*, *23*(1), 95-108.
686 Berghuijs, W., R. Woods, and M. Hrachowitz (2014), A precipitation shift from snow towards
687 rain leads to a decrease in streamflow, *Nat. Clim. Change*, *4*(7), 583-586.
688 Brown, R. D., and P. W. Mote (2009), The response of northern hemisphere snow cover to a
689 changing climate*, *Journal of Climate*, *22*(8), 2124-2145.
690 Cayan, D. R., E. P. Maurer, M. D. Dettinger, M. Tyree, and K. Hayhoe (2008), Climate change
691 scenarios for the California region, *Climatic change*, *87*, 21-42.
692 Christensen, L., C. L. Tague, and J. S. Baron (2008), Spatial patterns of simulated transpiration
693 response to climate variability in a snow dominated mountain ecosystem, *Hydrological*
694 *Processes*, *22*(18), 3576-3588.
695 Cooper, M. G., A. W. Nolin, and M. Safeeq (2016), Testing the recent snow drought as an
696 analog for climate warming sensitivity of Cascades snowpacks, *Environmental Research*
697 *Letters*, *11*(8), 084009.
698 Dettinger, M. (2011), Climate Change, Atmospheric Rivers, and Floods in California–A
699 Multimodel Analysis of Storm Frequency and Magnitude Changes, *JAWRA Journal of the*
700 *American Water Resources Association*, *47*(3), 514-523.
701 Dettinger, M. D., and D. R. Cayan (1995), Large-scale atmospheric forcing of recent trends
702 toward early snowmelt runoff in California, *Journal of Climate*, *8*(3), 606-623.
703 Dettinger, M. D., D. R. Cayan, M. K. Meyer, and A. E. Jeton (2004), Simulated hydrologic
704 responses to climate variations and change in the Merced, Carson, and American River basins,
705 Sierra Nevada, California, 1900–2099, *Climatic Change*, *62*(1-3), 283-317.
706 Eiriksson, D., M. Whitson, C. H. Luce, H. P. Marshall, J. Bradford, S. G. Benner, T. Black, H.
707 Hetrick, and J. P. McNamara (2013), An evaluation of the hydrologic relevance of lateral flow
708 in snow at hillslope and catchment scales, *Hydrological Processes*, *27*(5), 640-654.
709 Elder, K., J. Dozier, and J. Michaelsen (1988), Spatial and temporal variation of net snow
710 accumulation in a small alpine watershed, Emerald Lake basin, Sierra Nevada, California,
711 USA, *Annals of Glaciology*, *13*, 56-63.

712 Etchevers, P., E. Martin, R. Brown, C. Fierz, Y. Lejeune, E. Bazile, A. Boone, Y.-J. Dai, R.
713 Essery, and A. Fernandez (2004), Validation of the energy budget of an alpine snowpack
714 simulated by several snow models (SnowMIP project), *Annals of Glaciology*, *38*(1), 150-158.
715 Eyring, V., S. Bony, G. A. Meehl, C. A. Senior, B. Stevens, R. J. Stouffer, and K. E. Taylor
716 (2016), Overview of the Coupled Model Intercomparison Project Phase 6 (CMIP6)
717 experimental design and organization, *Geoscientific Model Development*, *9*(5), 1937-1958.
718 Flerchinger, G., W. Xaio, D. Marks, T. Sauer, and Q. Yu (2009), Comparison of algorithms for
719 incoming atmospheric long‐wave radiation, *Water Resources Research*, *45*(3).
720 Fry, J. A., G. Xian, S. Jin, J. A. Dewitz, C. G. Homer, Y. LIMIN, C. A. Barnes, N. D. Herold,
721 and J. D. Wickham (2011), Completion of the 2006 national land cover database for the
722 conterminous United States, *Photogrammetric Engineering and Remote Sensing*, *77*(9), 858-
723 864.
724 Fyfe, J. C., C. Derksen, L. Mudryk, G. M. Flato, B. D. Santer, N. C. Swart, N. P. Molotch, X.
725 Zhang, H. Wan, and V. K. Arora (2017), Large near-term projected snowpack loss over the
726 western United States, *Nature Communications*, *8*.
727 Girotto, M., S. A. Margulis, and M. Durand (2014a), Probabilistic SWE reanalysis as a
728 generalization of deterministic SWE reconstruction techniques, *Hydrological Processes*,
729 *28*(12), 3875-3895.
730 Girotto, M., G. Cortés, S. A. Margulis, and M. Durand (2014b), Examining spatial and temporal
731 variability in snow water equivalent using a 27 year reanalysis: Kern River watershed, Sierra
732 Nevada, *Water Resources Research*, *50*(8), 6713-6734.
733 Gleason, K. E., A. W. Nolin, and T. R. Roth (2017), Developing a representative snow-
734 monitoring network in a forested mountain watershed, *Hydrology and Earth System Sciences*,
735 *21*(2), 1137.
736 Gleick, P. H. (1987), The development and testing of a water balance model for climate impact
737 assessment: modeling the Sacramento basin, *Water Resources Research*, *23*(6), 1049-1061.
738 Gleick, P. H., and E. L. Chalecki (1999), The impacts of climate changes for water resources of
739 the Colorado and Sacramento-San Joaquin River basins, *JAWRA Journal of the American*
740 *Water Resources Association*, *35*(6), 1429-1441.
741 Godsey, S., J. Kirchner, and C. Tague (2013), Effects of changes in winter snowpacks on
742 summer low flows: case studies in the Sierra Nevada, California, USA, *Hydrological*
743 *Processes*.
744 Hamlet, A. F., and D. P. Lettenmaier (2007), Effects of 20th century warming and climate
745 variability on flood risk in the western US, *Water Resources Research*, *43*(6).
746 Howat, I. M., and S. Tulaczyk (2005), Climate sensitivity of spring snowpack in the Sierra
747 Nevada, *Journal of Geophysical Research: Earth Surface*, *110*(F4).
748 Hunsaker, C. T., T. W. Whitaker, and R. C. Bales (2012), Snowmelt runoff and water yield along
749 elevation and temperature gradients in California's Southern Sierra Nevada1, edited, Wiley
750 Online Library.
751 Huntington, J. L., and R. G. Niswonger (2012), Role of surface‐water and groundwater
752 interactions on projected summertime streamflow in snow dominated regions: An integrated
753 modeling approach, *Water Resources Research*, *48*(11).
754 Jepsen, S. M., N. P. Molotch, M. W. Williams, K. E. Rittger, and J. O. Sickman (2012),
755 Interannual variability of snowmelt in the Sierra Nevada and Rocky Mountains, United States:
756 Examples from two alpine watersheds, *Water Resources Research*, *48*(2).

Klein Tank, A., F. W. Zwiers, and X. Zhang (2009), Guidelines on analysis of extremes in a changing climate in support of informed decisions for adaptation, edited by C. D. a. Monitoring, p. 56, World Meteorological Organization.
Knowles, N., and D. R. Cayan (2002), Potential effects of global warming on the Sacramento/San Joaquin watershed and the San Francisco estuary, *Geophysical Research Letters*, *29*(18), 38-31-38-34.
Knowles, N., and D. R. Cayan (2004), Elevational dependence of projected hydrologic changes in the San Francisco estuary and watershed, *Climatic Change*, *62*(1-3), 319-336.
Knowles, N., M. D. Dettinger, and D. R. Cayan (2006), Trends in Snowfall versus Rainfall in the Western United States, *Journal of Climate*, *19*(18), 4545-4559.
Kobierska, F., T. Jonas, M. Zappa, M. Bavay, J. Magnusson, and S. M. Bernasconi (2013), Future runoff from a partly glacierized watershed in Central Switzerland: a two-model approach, *Advances in Water Resources*, *55*, 204-214.
Kobierska, F., T. Jonas, J. Magnusson, M. Zappa, M. Bavay, T. Bosshard, F. Paul, and S. M. Bernasconi (2011), Climate change effects on snow melt and discharge of a partly glacierized watershed in Central Switzerland (SoilTrec Critical Zone Observatory), *Applied Geochemistry*, *26, Supplement*(0), S60-S62.
Lehning, M., I. Völksch, D. Gustafsson, T. A. Nguyen, M. Stähli, and M. Zappa (2006), ALPINE3D: a detailed model of mountain surface processes and its application to snow hydrology, *Hydrological Processes*, *20*(10), 2111-2128.
Letcher, T. W., and J. R. Minder (2015), Characterization of the Simulated Regional Snow Albedo Feedback Using a Regional Climate Model over Complex Terrain, *Journal of Climate*, *28*(19), 7576-7595.
Lettenmaier, D. P., and T. Y. Gan (1990), Hydrologic sensitivities of the Sacramento‐San Joaquin River Basin, California, to global warming, *Water Resources Research*, *26*(1), 69-86.
Lettenmaier, D. P., A. W. Wood, R. N. Palmer, E. F. Wood, and E. Z. Stakhiv (1999), Water resources implications of global warming: A US regional perspective, *Climatic Change*, *43*(3), 537-579.
Liston, G. E., and K. Elder (2006), A Meteorological Distribution System for High-Resolution Terrestrial Modeling (MicroMet), *Journal of Hydrometeorology*, *7*(2), 217-234.
Liu, C., K. Ikeda, R. Rasmussen, M. Barlage, A. J. Newman, A. F. Prein, F. Chen, L. Chen, M. Clark, and A. Dai (2016), Continental-scale convection-permitting modeling of the current and future climate of North America, *Climate Dynamics*, 1-25.
López-Moreno, J. I., S. Fassnacht, J. Heath, K. Musselman, J. Revuelto, J. Latron, E. Morán-Tejeda, and T. Jonas (2013), Small scale spatial variability of snow density and depth over complex alpine terrain: Implications for estimating snow water equivalent, *Advances in Water Resources*, *55*, 40-52.
López-Moreno, J. I., et al. (2017), Different sensitivities of snowpacks to warming in Mediterranean climate mountain areas, *Environmental Research Letters*.
Luce, C. H., and Z. A. Holden (2009), Declining annual streamflow distributions in the Pacific Northwest United States, 1948–2006, *Geophysical Research Letters*, *36*(16).
Lundquist, J. D., and S. P. Loheide (2011), How evaporative water losses vary between wet and dry water years as a function of elevation in the Sierra Nevada, California, and critical factors for modeling, *Water Resources Research*, *47*(3).

Magnusson, J., D. Farinotti, T. Jonas, and M. Bavay (2011), Quantitative evaluation of different hydrological modelling approaches in a partly glacierized Swiss watershed, *Hydrological Processes*, *25*(13), 2071-2084.
Margulis, S. A., G. Cortés, M. Girotto, and M. Durand (2016), A Landsat-Era Sierra Nevada Snow Reanalysis (1985–2015), *Journal of Hydrometeorology*, *17*(4), 1203-1221.
Marks, D., and J. Dozier (1992), Climate and energy exchange at the snow surface in the alpine region of the Sierra Nevada: 2. Snow cover energy balance, *Water Resources Research*, *28*(11), 3043-3054.
Marks, D., J. Dozier, and R. E. Davis (1992), Climate and energy exchange at the snow surface in the Alpine Region of the Sierra Nevada: 1. Meteorological measurements and monitoring, *Water Resour. Res.*, *28*(11), 3029-3042.
Marty, C., S. Schlögl, M. Bavay, and M. Lehning (2017), How much can we save? Impact of different emission scenarios on future snow cover in the Alps, *The Cryosphere*, *11*(1), 517.
McCabe, G. J., and M. P. Clark (2005), Trends and variability in snowmelt runoff in the western United States, *Journal of Hydrometeorology*, *6*(4), 476-482.
Michlmayr, G., M. Lehning, G. Koboltschnig, H. Holzmann, M. Zappa, R. Mott, and W. Schöner (2008), Application of the Alpine 3D model for glacier mass balance and glacier runoff studies at Goldbergkees, Austria, *Hydrological Processes*, *22*(19), 3941-3949.
Minder, J. R. (2010), The Sensitivity of Mountain Snowpack Accumulation to Climate Warming, *Journal of Climate*, *23*(10), 2634-2650.
Molotch, N., M. Colee, R. Bales, and J. Dozier (2005), Estimating the spatial distribution of snow water equivalent in an alpine basin using binary regression tree models: the impact of digital elevation data and independent variable selection, *Hydrological Processes*, *19*(7), 1459-1479.
Molotch, N. P., and L. Meromy (2014), Physiographic and climatic controls on snow cover persistence in the Sierra Nevada Mountains, *Hydrological Processes*, *28*(16), 4573-4586.
Molotch, N. P., P. D. Blanken, M. W. Williams, A. A. Turnipseed, R. K. Monson, and S. A. Margulis (2007), Estimating sublimation of intercepted and sub-canopy snow using eddy covariance systems, *Hydrological Processes*, *21*(12), 1567-1575.
Mote, P. W., A. F. Hamlet, M. P. Clark, and D. Lettenmaier (2005), Declining mountain snowpack in western North America, *B Am Meteorol Soc*, *86*, 39-49.
Mott, R., F. Faure, oise, M. Lehning, H. we, B. Hynek, G. Michlmayer, A. Prokop, Sch, and W. ner (2008), Simulation of seasonal snow-cover distribution for glacierized sites on Sonnblick, Austria, with the Alpine3D model, *Annals of Glaciology*, *49*(1), 155-160.
Musselman, K. N., J. W. Pomeroy, R. L. Essery, and N. Leroux (2015), Impact of windflow calculations on simulations of alpine snow accumulation, redistribution and ablation, *Hydrological Processes*, *29*(18), 3983-3999.
Musselman, K. N., N. P. Molotch, S. A. Margulis, M. Lehning, and D. Gustafsson (2012a), Improved snowmelt simulations with a canopy model forced with photo-derived direct beam canopy transmissivity, *Water Resour. Res.*, *48*(10).
Musselman, K. N., N. P. Molotch, S. A. Margulis, P. Kirchner, and R. C. Bales (2012b), Influence of canopy structure and direct beam solar irradiance on snowmelt rates in a mixed conifer forest, *Agricultural and Forest Meteorology*, *161C*, 46-56.
Musselman, K. N., M. P. Clark, C. Liu, K. Ikeda, and R. Rasmussen (2017), Slower snowmelt in a warmer world, *Nature Clim. Change*, *7*(3), 214-219.

Nolin, A. W., and C. Daly (2006), Mapping “at risk” snow in the Pacific Northwest, *J Hydrometeorol*, *7*(5), 1164-1171.
NPS (2017), Sequoia and Kings Canyon National Park, Weather and Climate, edited.
Penna, D., H. J. Tromp-van Meerveld, A. Gobbi, M. Borga, and G. Dalla Fontana (2011), The influence of soil moisture on threshold runoff generation processes in an alpine headwater catchment, *Hydrol. Earth Syst. Sci.*, *15*(3), 689-702.
Pepin, N., and J. Lundquist (2008), Temperature trends at high elevations: patterns across the globe, *Geophysical Research Letters*, *35*(14).
Perrot, D., N. P. Molotch, M. W. Williams, S. M. Jepsen, and J. O. Sickman (2014), Relationships between stream nitrate concentration and spatially distributed snowmelt in high‐elevation catchments of the western US, *Water Resources Research*, *50*(11), 8694-8713.
Prein, A. F., R. M. Rasmussen, K. Ikeda, C. Liu, M. P. Clark, and G. J. Holland (2016), The future intensification of hourly precipitation extremes, *Nature Climate Change*.
Rasouli, K., J. W. Pomeroy, and D. G. Marks (2015), Snowpack sensitivity to perturbed climate in a cool mid‐latitude mountain catchment, *Hydrological Processes*, *29*(18), 3925-3940.
Rice, R., R. C. Bales, T. H. Painter, and J. Dozier (2011), Snow water equivalent along elevation gradients in the Merced and Tuolumne River basins of the Sierra Nevada, *Water Resources Research*, *47*(8).
Rutter, N., et al. (2009), Evaluation of forest snow processes models (SnowMIP2), *J Geophys Res-Atmos*, *114*, -.
Schlögl, S., C. Marty, M. Bavay, and M. Lehning (2016), Sensitivity of Alpine3D modeled snow cover to modifications in DEM resolution, station coverage and meteorological input quantities, *Environmental Modelling & Software*, *83*, 387-396.
Seager, R., M. Ting, C. Li, N. Naik, B. Cook, J. Nakamura, and H. Liu (2013), Projections of declining surface-water availability for the southwestern United States, *Nature Climate Change*, *3*(5), 482-486.
Sexstone, G. A., D. W. Clow, D. I. Stannard, and S. R. Fassnacht (2016), Comparison of methods for quantifying surface sublimation over seasonally snow‐covered terrain, *Hydrological Processes*, *30*(19), 3373-3389.
Sickman, J. O., A. Leydecker, C. C. Chang, C. Kendall, J. M. Melack, D. M. Lucero, and J. Schimel (2003), Mechanisms underlying export of N from high-elevation catchments during seasonal transitions, *Biogeochemistry*, *64*(1), 1-24.
Sproles, E. A., T. R. Roth, and A. W. Nolin (2017), Future snow? A spatial-probabilistic assessment of the extraordinarily low snowpacks of 2014 and 2015 in the Oregon Cascades, *The Cryosphere*, *11*(1), 331-341.
Stewart, I. T., D. R. Cayan, and M. D. Dettinger (2004), Changes in snowmelt runoff timing in western North America under abusiness as usual climate change scenario, *Climatic Change*, *62*(1-3), 217-232.
Stocker, T. F., D. Qin, G.-K. Plattner, M. Tignor, S. K. Allen, J. Boschung, A. Nauels, Y. Xia, V. Bex, and P. M. Midgley (2013), Climate Change 2013. The Physical Science Basis. Working Group I Contribution to the Fifth Assessment Report of the Intergovernmental Panel on Climate Change-Abstract for decision-makers, Groupe d'experts intergouvernemental sur l'evolution du climat/Intergovernmental Panel on Climate Change-IPCC, C/O World Meteorological Organization, 7bis Avenue de la Paix, CP 2300 CH-1211 Geneva 2 (Switzerland).

892 Sturm, M., M. A. Goldstein, and C. Parr (2017), Water and life from snow: A trillion dollar
893 science question, *Water Resources Research*.
894 Sun, F., A. Hall, M. Schwartz, D. B.Walton, and N. Berg (2016), Twenty-First-Century Snowfall
895 and Snowpack Changes over the Southern California Mountains, *Journal of Climate*, *29*(1),
896 91-110.
897 Tague, C., and H. Peng (2013), The sensitivity of forest water use to the timing of precipitation
898 and snowmelt recharge in the California Sierra: Implications for a warming climate, *Journal*
899 *of Geophysical Research: Biogeosciences*, *118*(2), 875-887.
900 Tague, C., G. Grant, M. Farrell, J. Choate, and A. Jefferson (2008), Deep groundwater mediates
901 streamflow response to climate warming in the Oregon Cascades, *Climatic Change*, *86*(1-2),
902 189-210.
903 Tonnessen, K. A. (1991), The Emerald Lake watershed study: introduction and site description,
904 *Water Resour. Res.*, *27*(7), 1537-1539.
905 Trenberth, K. E. (2011), Changes in precipitation with climate change, *Climate Research*, *47*(1-
906 2), 123-138.
907 Trujillo, E., and N. P. Molotch (2014), Snowpack regimes of the Western United States, *Water*
908 *Resources Research*, *50*(7), 5611-5623.
909 Trujillo, E., and M. Lehning (2015), Theoretical analysis of errors when estimating snow
910 distribution through point measurements, *The Cryosphere*, *9*(3), 1249-1264.
911 Trujillo, E., N. P. Molotch, M. L. Goulden, A. E. Kelly, and R. C. Bales (2012), Elevation-
912 dependent influence of snow accumulation on forest greening, *Nature Geoscience*, *5*(10), 705-
913 709.
914 Van Oldenborgh, G., M. Collins, J. Arblaster, J. Christensen, J. Marotzke, S. Power, M.
915 Rummukainen, T. Zhou, T. Stocker, and D. Qin (2013), Annex I: Atlas of global and regional
916 climate projections, *Climate change*, 1311-1393.
917 Vano, J. A., B. Udall, D. R. Cayan, J. T. Overpeck, L. D. Brekke, T. Das, H. C. Hartmann, H. G.
918 Hidalgo, M. Hoerling, and G. J. McCabe (2014), Understanding uncertainties in future
919 Colorado River streamflow, *Bulletin of the American Meteorological Society*, *95*(1), 59-78.
920 West, A. J., and K. R. Knoerr (1959), Water losses in the Sierra Nevada, *Journal (American*
921 *Water Works Association)*, *51*(4), 481-488.
922 Williams, M. W., and J. M. Melack (1991), Solute chemistry of snowmelt and runoff in an alpine
923 basin, Sierra Nevada, *Water resources research*, *27*(7), 1575-1588.
924 Winchell, T. S., D. M. Barnard, R. K. Monson, S. P. Burns, and N. P. Molotch (2016), Earlier
925 snowmelt reduces atmospheric carbon uptake in midlatitude subalpine forests, *Geophysical*
926 *Research Letters*, *43*(15), 8160-8168.

927

Tables

Table 1. Meteorological station and snow measurement details. Station numbers are ranked by station elevation and correspond to those mapped in Fig. 1. The variables measured at each location are listed: air temperature (Ta), relative humidity (RH), wind speed (ws), precipitation (ppt), snow water equivalent (SWE), and snow depth (depth).

#	Station name	Elev., m	Measured variables*	Operating agency
Automated met. stations				
1	D0117	263	Ta, RH, ws	APRSWXNET
2	C4177	378	Ta, RH, ws	APRSWXNET
3	Ash Mountain	527	Ta, RH, ws, ppt	NPS
4	Shadequarter	1323	Ta, RH, ws	CDF
5	Wolverton	1598	Ta, RH, ws	NPS
6	Lower Kaweah	1926	Ta, RH, ws, ppt	NPS
7	Atwell	1951	ppt	USACE
8	Case Mountain	1967	Ta, RH, ws	BLM
9	Giant Forest	2027	Ta, ppt	USACE
10	Bear Trap Meadow	2073	ppt	USACE
11	Wolverton Meadow	2229	Ta, RH, ws	SNRI
12	Park Ridge	2299	Ta, RH, ws	NPS
13	Hockett Meadows	2592	ppt	USACE
14	Marble Fork	2626	Ta	ERI
15	Panther Meadow	2640	Ta, RH, ws	SNRI
16	Emerald Lake	2835	Ta, RH, ws	ERI
17	Farewell Gap	2896	Ta	USACE
18	Topaz Lake	3232	Ta, RH, ws, SW, LW	ERI
19	M3	3288	Ta, RH, ws	ERI
Automated snow stations				
20	Giant Forest	1951	SWE	USACE
21	Big Meadows	2317	SWE	USACE
22	Farewell Gap	2896	SWE, depth	USACE
Monthly snow courses				
23	Giant Forest	1951	SWE, depth	NPS
24	Big Meadows	2317	SWE, depth	CADWP
25	Mineral King	2439	SWE, depth	NPS
26	Hockett Meadow	2592	SWE, depth	NPS
27	Panther Meadow	2622	SWE, depth	NPS
28	Rowell Meadow	2698	SWE, depth	KRWA
29	Scenic Meadow	2942	SWE, depth	KRWA

*Meteorological variables used in this study.
APRSWXNET: Automatic Position Reporting System as a Weather NETwork
NPS: National Park Service (Sequoia and Kings Canyon National Parks)
CDF: California Department of Forestry
USACE: United States Army Corps of Engineers
BLM: Bureau of Land Management
SNRI: Sierra Nevada Research Institute, University of California Merced
ERI: Earth Research Institute, University of California Santa Barbara
CADWP: California Department of Water and Power
KRWA: Kaweah River Water Association

Keith Musselman 10/13/2017 2:59 PM
Deleted: 1

Keith Musselman 10/13/2017 2:59 PM
Deleted: 3

Keith Musselman 10/13/2017 2:59 PM
Deleted: 1

Keith Musselman 10/13/2017 2:59 PM
Deleted: 2

Keith Musselman 10/13/2017 2:59 PM
Deleted: 3

Keith Musselman 10/13/2017 2:59 PM
Deleted: 4

Keith Musselman 10/13/2017 2:59 PM
Deleted: 5

Keith Musselman 10/13/2017 2:59 PM
Deleted: 6

Keith Musselman 10/13/2017 2:59 PM
Deleted: 7

952 Table 2. Average (hourly) air temperature and shortwave radiation values measured at the alpine
953 Topaz Lake meteorological station in the Tokopah Basin for JFM and AMJ of the moderately
954 dry year (2009), near-average year (2008) and moderately wet year (2010).

	Air temperature, °C		Shortwave, W m^{-2}	
	JFM	AMJ	JFM	AMJ
2009	-3.2	3.3	163	279
2008	-3.6	3.4	166	317
2010	-4.0	1.3	152	306

955

Table 3. Mean daily values of hourly measured meteorological variables (nominal mean) during the three mid-winter melt events in 2009 (see Fig. 10) compared to the average conditions measured at eight stations > 2250 m asl computed on 11-days centered on the event dates, averaged over the three years of the study. Precipitation is reported as the daily sum of measured values. Melt rates simulated in the nominal case are reported as the mean value computed over all grid elements > 2250 m asl and the maximum value over the full domain with the corresponding elevation.

Met. variable	Jan. 21	Feb. 22	Mar. 1
Air temp., °C	2.8 / -0.5	-0.7 / 0.6	4.4 / 1.0
Shortwave, W m^{-2}	57 / 96	83 / 152	163 / 176
Longwave, W m^{-2}	292 / 232	297 / 226	266 / 217
Wind, m s^{-1}	4.0 / 4.3	4.6 / 4.0	7.2 / 4.4
Precipitation, mm	0.0	4.3	0.0
Mean melt rate, mm d^{-1} nom. sim. (>2250 m)	6.5	1.5	4.7
Max. melt rate, mm d^{-1} nom. sim. (elev., m)	30.6 (1897)	28.3 (1586)	44.0 (1741)

Figures

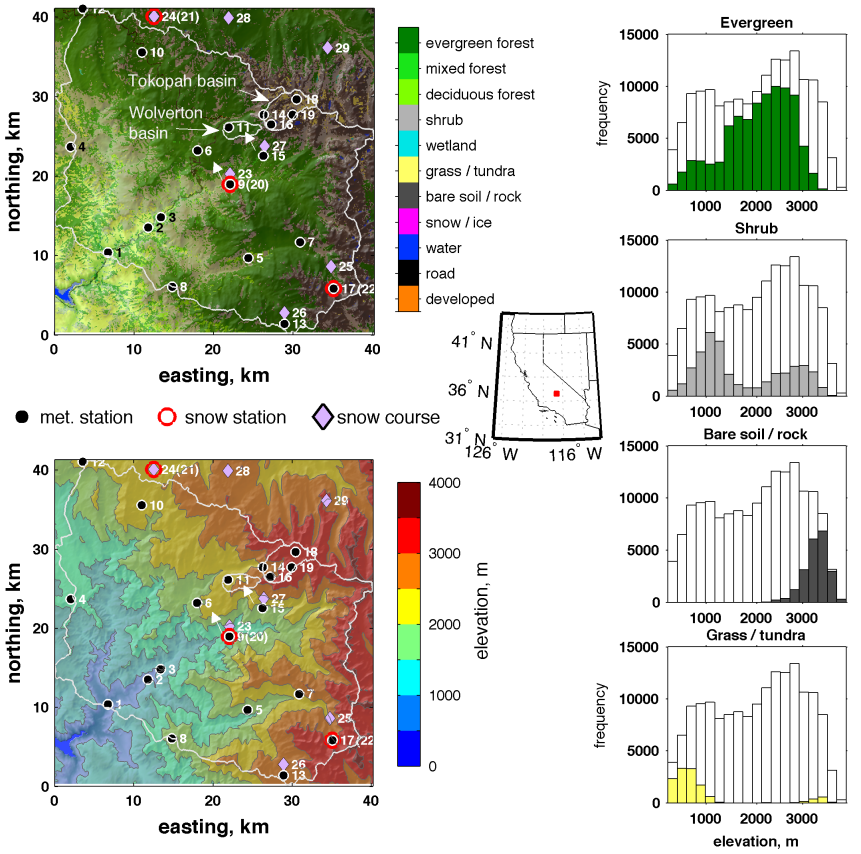

Figure 1: The elevation and land cover distribution of the model domain encompassing the Kaweah River basin (outlined) on the western side of the southern Sierra Nevada, California. Locations of the forested Wolverton and largely alpine Tokopah research basins are indicated. The locations of 19 automated meteorological stations (filled circle markers), three automated snow stations (red circles), and, seven monthly snow survey transects (diamond markers) are shown. Station numbers, ranked by elevation, correspond to those in Table 1. The histograms illustrate the elevation distribution of the four primary land cover types (colored bars) relative to the elevation of the model domain (empty bars).

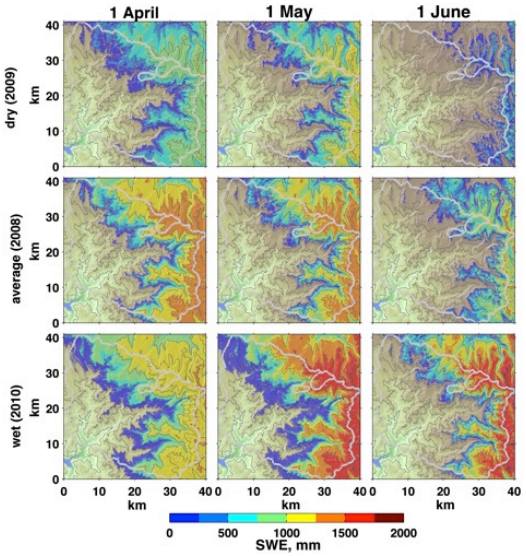

Figure 2: Simulated SWE over the greater Kaweah River basin on the first of April (left panel column), May (center panel column), and June (right panel column) for a moderately dry water year (2009; top panel row), near-climatological-average water year (2008; middle panel row), and a moderately wet water year (2010; bottom panel row).

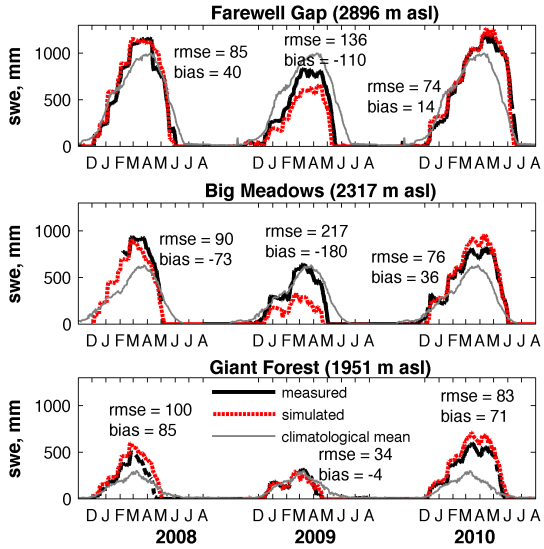

Figure 3: Measured and simulated SWE at the three automated snow stations spanning the middle elevations of the greater Kaweah River basin. The error metrics RMSE and bias, in millimeters, are provided for each station-year. The thin gray line indicates the long-term climatological mean SWE based on 26-years of data (1988 – 2014) collected at the Giant Forest and Big Meadows stations and a 15-year record (2000 – 2014) at the Farewell Gap station.

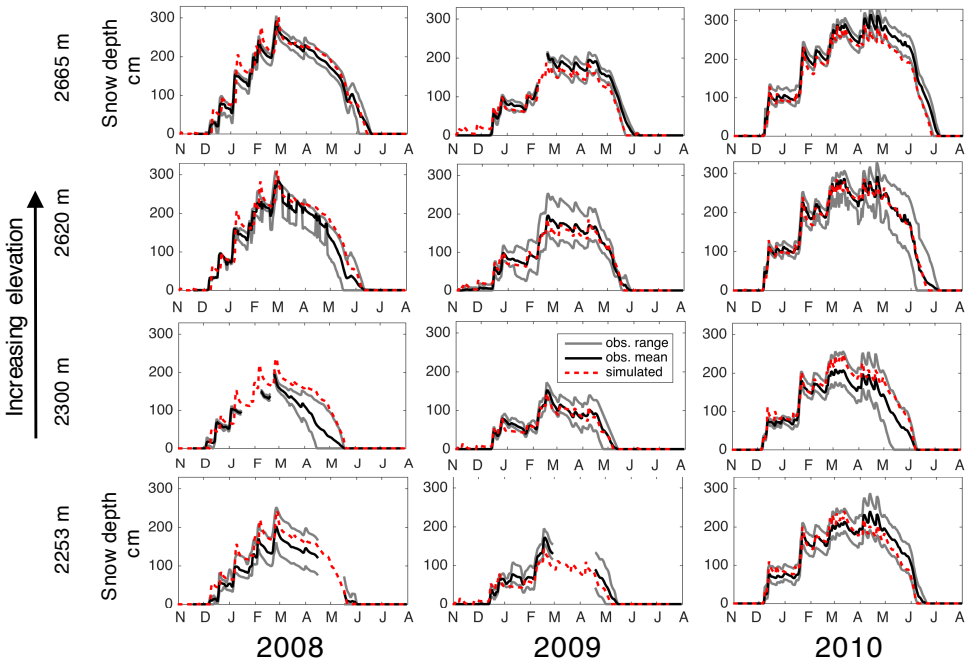

Figure 4: Comparison of three years (panel columns) of daily (x-axes) simulated (red lines) snow depth and the six-sensor observed range (gray lines) and mean (bold lines) snow depth measured by automated sensors at four research sites (panel rows) at different elevations in the Wolverton basin.

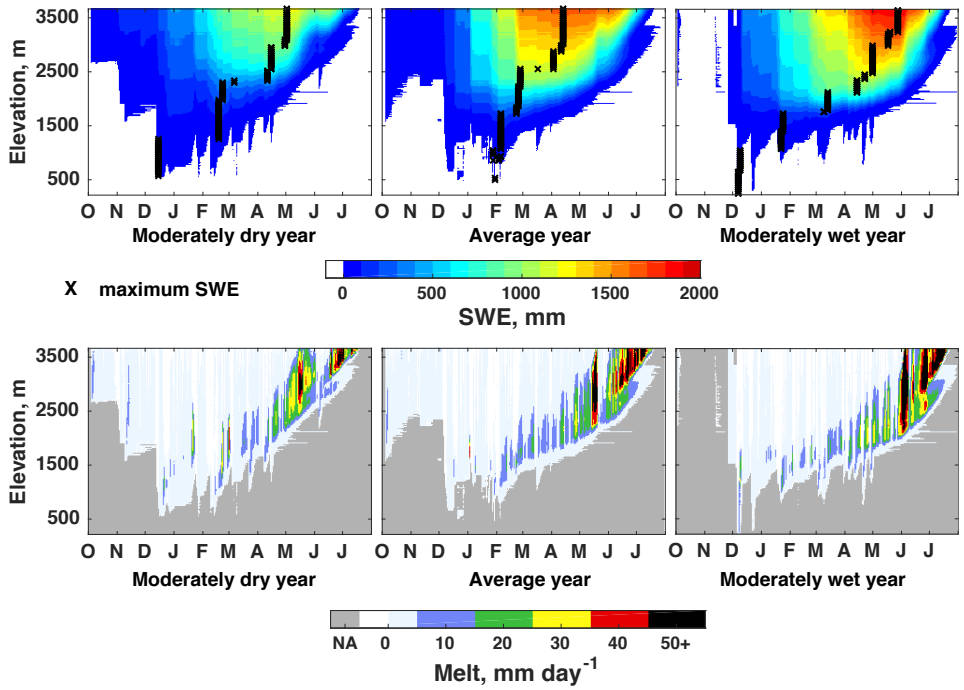

Figure 5: Distribution of (top panels) SWE and (bottom panels) daily melt by elevation (mean values within 18 m elevation bins; y-axes) and time (daily; x-axes) for a moderately dry (2009; left column panels), near-average (2008; center column panels), and moderately wet (2010; right column panels) snow season. The grey color in the lower panels indicates times when there is no snow to melt (NA). The elevation-specific dates of maximum SWE are indicated.

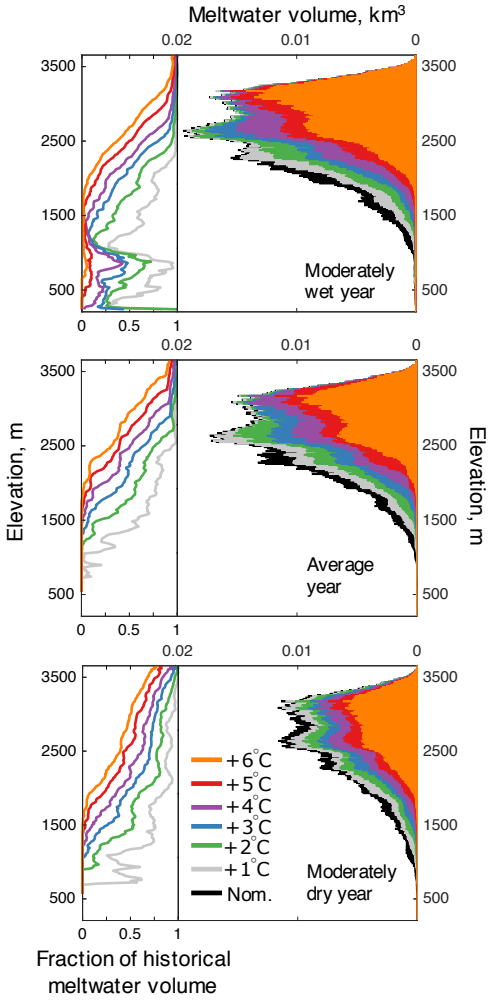

Figure 6: The elevation distribution (y-axes) of (right bar graphs) simulated annual meltwater volume and (line graphs) the fraction of that historical meltwater for each warmer scenario (colors; see legend) for the (top) moderately wet, (middle) average, and (bottom) moderately dry snow seasons. The total meltwater was summed within the same elevation bins used in Fig. 5.

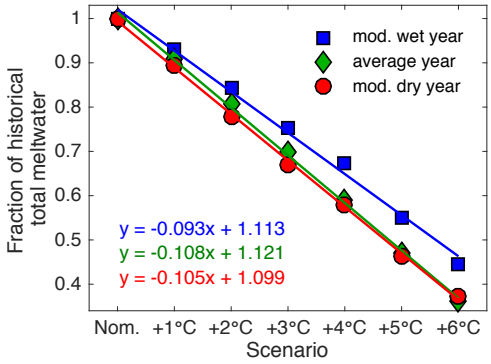

Figure 7: The fraction of simulated domain-wide historical meltwater (y-axis), relative to the nominal case, for each warmer temperature scenario (x-axis) for the three years (marker type and color). The colored lines and associated regression equations show linear fits to the data. For each year, the R^2 value was > 0.99 and the p-value was $\ll$ 1e-6.

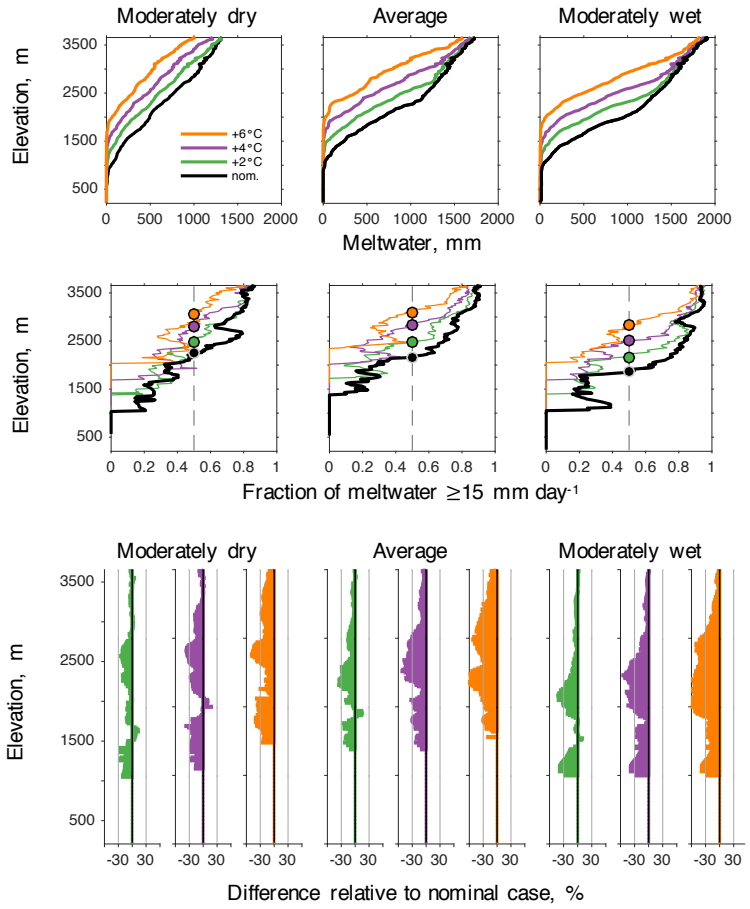

Figure 8: The elevation distribution (y-axes) of (top row of panels) the average total depth of annual meltwater (x-axes) simulated for the nominal case (black lines) and select perturbed temperature scenarios (colored lines), and (second row of panels) the fraction of annual meltwater produced at snowmelt rates ≥15 mm day^{-1}. The colored circles indicate elevations at which simulated melt occurs equally at rates ≥15 mm day^{-1} and <15 mm day^{-1}. The lower panels of colored graphs show the differences from the nominal case, reported in percent of annual meltwater, produced at snowmelt rates ≥15 mm day^{-1} for the three select scenarios. Results are shown for the moderately dry (2009; left column of plots), near-average (2008; middle column of plots), and moderately wet (2010; right column of plots) snow seasons.

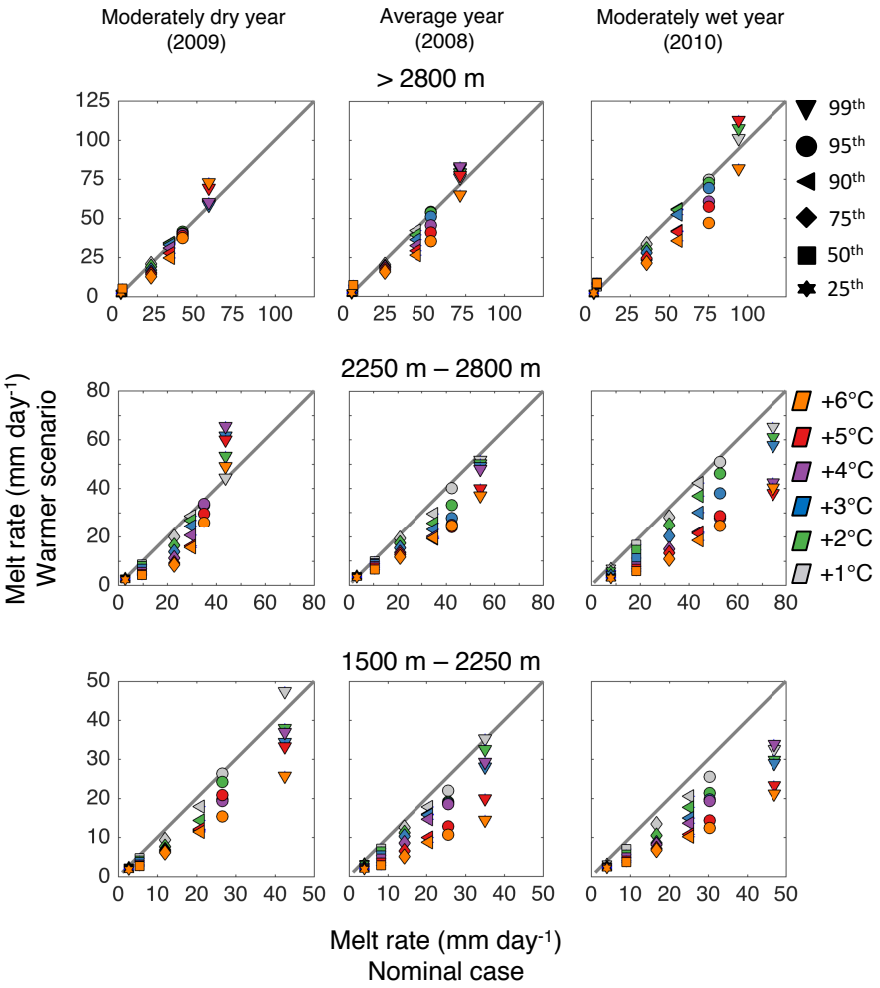

Figure 9: Quantile plots of simulated melt rates for the nominal (x-axes) and warmer scenarios (y-axes) for model grid cells characterized as high elevation (> 2800 m; top row of panels), middle elevation (2250 m – 2800 m; middle row of panels) and lower elevation (1500 m – 2250 m) regions for the moderately dry year (left column), average year (middle column) and moderately wet year (right column). Marker colors correspond to the six different temperature perturbations. Plotted in each graph are the 25th, 50th, 75th, 90th, 95th, and 99th percentiles (marker shapes) of daily snowmelt rates ≥ 1 mm day^{-1} for all grid cells within each water year and elevation range. The 1:1 lines are plotted for reference.

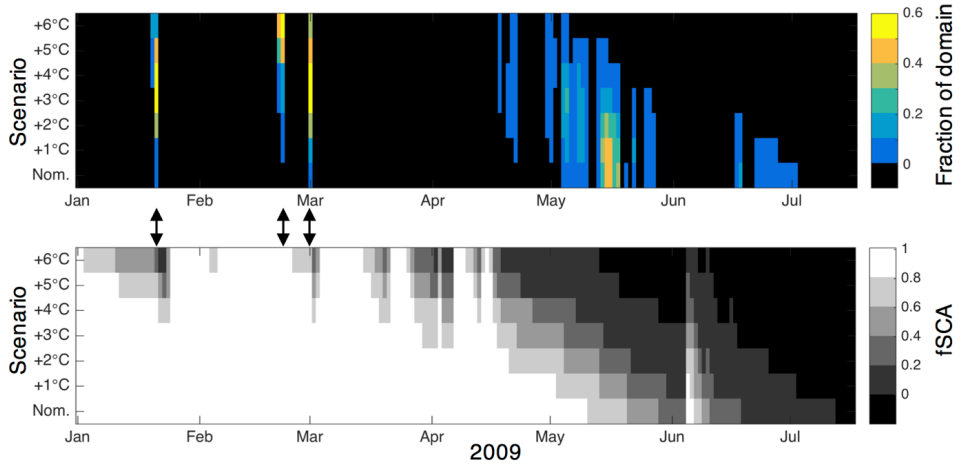

Figure 10: Daily extreme snowmelt in 2009 (melt rates > 40 mm day^{-1} at model grid cells > 2250 m asl, corresponding to extreme melt rates [≥ 99th percentile]; see Fig. 8) as simulated by the nominal (Nom.) and six perturbed temperature scenarios (y-axes) shown as the (top panel) fraction of the area undergoing extreme melt. The lower panel shows the fraction of snow-covered area (fSCA) for the same time period and domain. Arrows indicate (winter) melt events (see Table 3 for meteorological conditions and averages).